J. Astrophys. Astr. (1997) **18**, 91–131

On the Polarisation and Emission Geometry of Pulsar 1929+10: Does Its Emission Come from a Single Pole or Two Poles?

Joanna M. Rankin, *Physics Department, University of Vermont, Burlington, Vermont 05405 USA*

N. Rathnasree *Raman Research Institute Bangalore 560 080 India*

Received 1996 November 21; accepted 1997 June 24

Abstract. Pulsar B1929+10 is remarkable on a number of grounds. Its narrow primary components exhibit virtually complete and highly stable linear polarisation, which can be detected over most of its rotation cycle. Various workers have been lured by the unprecedented range over which its linear polarisation angle can be determined, and more attempts have been made to model its emission geometry than perhaps for any other pulsar. Paradoxically, there is compelling evidence to interpret the pulsar's emission geometry *both* in terms of an aligned configuration whereby its observed radiation comes from a single magnetic-polar emission region *and* in terms of a nearly orthogonal configuration in which we receive emission from regions near each of its two poles. Pulsar 1929+10 thus provides a fascinating context in which to probe the conflict between these lines of interpretation in an effort to deepen our understanding of pulsar radio emission.

Least-squares fits to the polarisation-angle traverse fit poorly near the main pulse and interpulse and have an inflection point far from the centre of the main pulse. This and a number of other circumstances suggest that the position-angle traverse is an unreliable indicator of the geometry in this pulsar, possibly in part because its low level 'pedestal' emission makes it impossible to properly calibrate a polarimeter which correlates orthogonal circular polarisations.

Taking the interpulse and main-pulse comp. II widths as indicators of the magnetic latitude, it appears that pulsar 1929+10 has an α value near 90° and thus has a two-pole interpulse geometry. This line of interpretation leads to interesting and consistent results regarding the geometry of the conal components. Features corresponding to both an inner and outer cone are identified. In addition, it appears that pulsar 1929+10—and a few other stars—have what we are forced to identify as a 'further-in' cone, with a conal emission radius of about $2.3°/P^{\frac{1}{2}}$.

Secondarily, 1929+10's nearly complete linear polarisation provides an ideal opportunity to study how mechanisms of depolarisation function on a pulse-to-pulse basis. Secondary-polarisation-mode emission appears in significant proportion only in some limited ranges of longitude, and the subsequent depolarization is studied using different mode-separation techniques. The characteristics of the two polarisation modes are particularly interesting, both because the primary mode usually dominates the

secondary so completely and because the structure seen in the secondary mode appears to bear importantly on the question of the pulsar's basic emission geometry. New secondary-mode features are detected in the average profile of this pulsar which appear independent of the main-pulse component structure and which apparently constitute displaced modal emission.

Individual pulses during which the secondary-mode dominates the primary one are found to be considerably more intense than the others and largely depolarised. Monte-Carlo modeling of the mode mixing in this region, near the boundary of comps. II and III, indicates that the incoherent interference of two fully and orthogonally polarised modes can adequately account for the observed depolarisation. The amplitude distributions of the two polarisation modes are both quite steady: the primary polarisation mode is well fitted by a χ^2 distribution with about nine degrees of freedom; whereas the secondary mode requires a more intense distribution which is constant, but sporadic.

Key words. Pulsars—polarisation—PSR B1929+10.

1. Introduction

Pulsar B1929+10 was among the first few pulsars discovered (Large, Vaughan & Wielebinski 1968) in the initial international fervour of searches following the announcement of the first four Cambridge pulsars (Hewish *et al.* 1968; Pilkington *et al.* 1968). With a period of 0.227 s, it was for a time the fastest known pulsar, and its dispersion measure (DM) of $\sim$3.18 pc/cm^3 placed it closer to the Sun than any pulsar apart from 0950+08.[1] Subsequent study showed that it had a spindown value of $\sim 1.16 \times 10^{-15}$ sec/sec—giving it a B_{12}/P^2 value of 10.1; we shall say more about the significance of this below.

Working at Arecibo, Craft (1969) soon discovered that the pulsar had an interpulse (IP)[2] with an amplitude of about 2% that of the main pulse (MP). This discovery was then followed much later by Perry & Lyne's (1985) identification of what they also called an 'interpulse' following the MP about midway between the MP and IP. This feature is nearly 10 times weaker in amplitude, but much broader than the IP. In order to avoid confusion, we will refer to this component as the 'postcursor' (PC). Using interferometry at 408 MHz, these authors also discovered that part of 1929+10's emission is continuous; the pulsed emission sits on a 'pedestal' of continuous emission with a relative amplitude somewhat less than that of the PC—that is, $0.151 \pm 0.016\%$ of the MP peak. Hankins & Fowler (1986) made a comprehensive

[1] Two pulsars with smaller DM values are now known: the millisecond pulsar J0437-4715 with a DM value of 2.65 pc/cm^3 and the 0.8-s pulsar J0108-1431 (Tauris *et al.* 1994) with a DM of 1.85 pc/cm^3.

[2] The term 'interpulse' is here used to mean a secondary region of emission, comparable to the main-pulse region, but separated from it in longitude by something like half a rotation cycle. 'Interpulsar' then denotes a pulsar with such an interpulse. This usage is usual among radio astronomers who study pulsars; we are aware, however, that the high-energy community uses the term to mean weak emission between pulses.

study of 1929+10's IP and determined that it follows the MP by $187.4 \pm 0.2°$ at 1 GHz and that its position is virtually independent of radio frequency. This study also shows the PC and yet another feature on the trailing edge of the MP; see their figures 2(c) and 3.

The frequency evolution of the MP also attracted early attention. Backer (1976) identified it as having three profile components—and thus placed it in his triple (T) class. This was not straightforward as the three components are so closely spaced that in some frequency bands only two features are apparent. The subtlety of pulsar 1929+10's profile structure is well illustrated in Hankins & Rickett's (1986) figure 1(i), where five total-power observations spanning the range between 277 and 2380 MHz are given.[3] At high frequencies the pulsar is among the very few detectable at 33.9 GHz (Wielebinski *et al.* 1993), and a 14.8-GHz profile has long been available (Bartel, Sieber & Wielebinski 1978). Despite the pulsar's small DM, it is not strong at low frequencies; Izvekova, Malofeev & Shitov (1989) have published a profile at 102 MHz, but it is only barely detectable using Arecibo at 50 MHz (Hankins & Rankin 1994).[4]

As noted in Paper III, the published studies of 1929+10's fluctuation properties raise as many questions as they answer. Overall, the pulsar is rather steady, meaning that most individual pulses nominally resemble the average profile and do not vary drastically in intensity [see Taylor *et al.* (1975); figure 3]. Backer (1970), however, while looking for nulling phenomena, first noted a pattern of *weak* pulses in '6s and 12s', and although he referred to these as 'null' pulses, no subsequent study has identified a true population of null pulses according to the usual criteria (Ritchings 1976). Subsequent studies both by Backer (1973) and others (Taylor & Huguenin 1971; Taylor *et al.* 1975; Nowakowski *et al.* 1982) confirm broad 'red' features between 0.05 and 0.12 cycles/period peaking consistently at about 0.09 cycles/period or a P_3 of 11.6 periods. Pulsar 1929+10 is the only pulsar we know of where fluctuation-spectrum features are reportedly associated with a population of *weak* pulses rather than strong ones.

The large fractional linear polarisation of pulsar 1929+10 was noted very early (Manchester *et al.* 1973). It provided a second example (after 0833–45) of a pulsar whose fractional linear polarisation remains high over the entire frequency range that it can be observed.[5] As with most pulsars 1929+10's fractional linear gradually decreases at high frequency. Recent Bonn polarimetry, however, shows that it reaches 60% even at 10.55 GHz (Xilouris *et al.* 1995).

Full period, average polarimetry has been published for 1929+10 at 430 MHz (Rankin & Benson 1981), 1400 MHz (Rankin, Stinebring & Weisberg 1989; and

[3] Sieber *et al.* (1975) have studied the evolution of the pulsar's profile quantitatively—obtaining a frequency dependence for the separation of its *two* components of $f^{-0.28}$—but they seem to have misaligned the 430-MHz profile with those at higher frequencies, so that they consider (in our terms) components II and III at 430 MHz and then I and II at higher frequencies! An intermediate frequency profile at 800 MHz is given by Stinebring *et al.* (1984b) and clearly shows the three components.

[4] This detection involved integrating for more than two hours and dedispersing over a 312-kHz bandwidth with a resolution of just over 1° of longitude. The feed sensitivity was probably about 5 K/Jy.

[5] This was then all the more remarkable because early polarimeters often 'lost' some polarisation through non-orthogonality or instrumental position-angle rotation across the passband.

Blaskiewicz, Cordes & Wasserman 1991), and 2650 MHz (Morris *et al.* 1981). Individual-pulse polarimetric studies have been carried out at 430 MHz (Backer & Rankin 1980), 800 MHz (Stinebring *et al.* 1984b) and 1400 MHz (Stinebring *et al.* 1984a). Throughout this frequency range the linear polarisation of the MP and IP are both very large, and there is usually a little negative circular polarisation associated with the MP. As might be expected for such a pulsar, individual-pulse sequences show rather little variation in polarisation from pulse to pulse. Indeed, pulsar 1929+10 has the highest and most consistent polarisation of any known pulsar (with the probable exception of the Vela pulsar); for this reason it is by far the most useful calibrator for polarisation measurements accessible to the Arecibo instrument (Rankin, Rathnasree & Xilouris 1998).

With emission coming from not only the MP, but from the IP and PC as well, the linear polarisation angle (PA) can be measured over an unprecedentedly large part of the star's rotation cycle. Some indication of this can be seen in Rankin & Benson's figure 3 and Rankin *et al.*'s figure 22, but much more graphic displays are found in Blaskiewicz *et al.*'s figure 22 and Phillip's (1990) figures 2 and 3. At 430 MHz, the PA can be measured over some 300° of longitude and at 1400 MHz or so, up to about 180°! Through use of these observations and the single-vector model (Radhakrishnan & Cooke 1969; Komesaroff 1970), a number of efforts have been made to determine the pulsar's emission geometry. The most salient feature of these PA traverses is that they are *very* shallow—about $-1.5^{\circ}/^{\circ}$ for the MP and $+0.6^{\circ}/^{\circ}$ for the IP. Using the data from Rankin & Benson, Narayan & Vivekanand (1982) found that α, the angle between the magnetic and rotational axes, was 35°, while β, the impact angle of the sight line, was +23° for the MP and +87° for the IP. Referencing the same observations, Lyne & Manchester (1988) came to the conclusion that α was about 15° and that the respective MP and IP β values were 7.5° and −37.5°.

Two different studies about two years later, each based on new, independent, Arecibo dual-frequency observations attempted to redetermine the emission geometry of 1929+10. Phillips' work was carried out at 430 and 1665 MHz, and he found α to be $30 \pm 2°$ and $35 \pm 4°$ and β $20 \pm 2°$ and $21 \pm 3°$ at the two frequencies, respectively. Blaskiewicz *et al.* using a relativistic model of the PA traverse, again determined values not far different from those of the previous studies; α was found to be $25 \pm 2°$ and $27 \pm 2°$ and β $16 \pm 2°$ and $16 \pm 3°$ at 430 and 1418 MHz, respectively. The values stemming from these studies are summarized in Table 1.

Table 1. Position-angle fitting results for pulsar 1929 + 10.

Source	α	β_{MP}	β_{IP}	f (MHz)
Narayan & Vivekanand (1982)	35°	23°	87°	430
Lyne & Manchester (1988)	15° (6°)	7.5° (4°)	−37.5°	430
Phillips (1990)	30° ± 2°	20° ± 2°	[80°]	430
	35° ± 4°	21° ± 3°	[91°]	1665
Blaskiewicz *et al.* (1991)	25° ± 2°	16° ± 2°		430
	27° ± 4°	16° ± 2°		1418
	30° ± 10°	3° ± 2°		1418
This paper	31°	20°		430

Needless to say, all of these studies concur in placing pulsar 1929+10 squarely in the category of single-pole interpulsars. In this view, the magnetic axis can at most be some 35° from the rotation axis, so that the MP would be produced by a cut through the emission region associated with one of the magnetic poles and the IP by another cut about half a rotation cycle later through a weaker region of emission associated with the same magnetic pole. This geometry is well illustrated by Phillips' (1990) figure 4.

Very different expectations about the emission geometry of pulsar 1929+10 have come from attempts to classify it. Following Backer (1976) it was classified provisionally as triple (**T**) in Paper III, noting that its subpulse modulation was more core-like than conal. Paper IV attempted to distinguish one- and two-pole interpulsars, and, despite the evidence (noted above) to the contrary, argued that it was probably a two-pole interpulsar on the basis of its narrow components and large value of B_{12}/P^2. The latter places the pulsar in the upper-left region of the period-spindown diagram, in which pulsars with core-emission-dominated profiles are the rule. Therefore, we should expect to identify core components in the pulsar's MP region, its IP region, or both. Apparently, both the primary IP feature and the central component (II) of the MP are core components. The former's width, measured accurately and interpolated to 1 GHz is *exactly* $2.45°/P^{\frac{1}{2}}$, the angular width of the polar cap, making the inferred magnetic latitude angle α essentially 90° and strongly implying that the emission geometry corresponds to that of a two-pole interpulsar. The putative MP core component (II) also has very nearly this same width; it is certainly no greater than that of the IP, but its width cannot be measured so accurately, due to the proximity of the conal components around it.

The effort in Paper VI (Rankin 1993a, b) to understand the conal geometry implied by pulsar emission profiles inherited this dilemma. The nearly 200 pulsars considered in this study were found to have conal emission beams with *very* regular properties. Some pulsars have 'inner' cones with angular diameters $\rho_{\rm inner}$ of $4.33°/P^{\frac{1}{2}}$, others have 'outer' cones with $\rho_{\rm outer}$ $5.75°/P^{\frac{1}{2}}$, and a third group have profiles with both types of cones. *Pulsar* 1929+10 *was virtually the only well studied pulsar of any profile class which could not be comfortably fitted into this quantitative description of the conal emission geometry.*

Initially, 1929+10 was viewed as a triple (**T**) pulsar; this is shown in Paper VI, Table 5. The magnetic latitude α was taken as 90° on the basis of the width of the interpulse (and MP comp. II). The shallow PA traverse ($|\Delta\chi/\Delta\phi|$) then implies that β is some 42°, which in turn also makes the radius of the conal emission beam ρ about 42°. Reference to Paper VI, Table 5 will show that no other pulsar has a ρ value remotely this large; if 1929+10 had an outer cone, its conal emission beam radius would be no more than some 12°. No other set of assumptions seems able to repair this discrepancy; even with the assumption—against all the PA-traverse evidence—that our sight line actually makes a central traverse across the core and conal beams, the resulting ρ value of 6.6° (= 13.2°/2) is now *smaller* than that of an inner cone—that is, $2 \times 4.33°/P^{\frac{1}{2}}$ or some 9.1°. One other desperate attempt to reconcile the pulsar's geometry with that of other pulsars is given in Paper VI, Table 6, where the assumption is made that it is a conal triple (c**T**) pulsar with an α value of about 18°. Here, finally, the dimensions of the outer cone come out about right, but the model dimension of the inner cone (assumed here to be comp. II) is much too large—and, of course, the interpulse geometry is problematic here no matter which way one jumps:

if the IP emission comes from the same pole, then the IP's narrow width is anomalous; if it comes from the other pole, then the IP's impact angle must be some 130°!!

Our principle task in this paper is then to understand pulsar 1929+10's emission geometry. Is this pulsar really different from the so many others which have such consistent angular dimensions of their core and conal emission beams? And if so, why? To this end, we shall introduce some new observational evidence, and therefore, in the next section we describe the characteristics of these new observations which will be used below in our analysis. In Section 3 we take a new look at the properties of the MP profile, and in Section 4 we present new, sensitive, full period polarisation measurements.

A second task is that of understanding pulsar 1929+10's high linear polarisation and the polarisation-modal construction of its average profile. Thus, in Sections 5 and 6 we explore several polarisation-mode separation techniques as applied to this pulsar, and in Section 7 we discuss how the two polarisation modes combine to configure the pulsar's profile. This will, in turn, shed some new light on the conal emission geometry.

In Section 8 we return to the significance of 1929+10's PA traverse and the overall question of its emission geometry, and in Section 9 we explore the implications of the displaced modal emission in the pulsar's profile. Section 10 explores how the pulsar's PA traverse might be distorted; and finally, in Sections 11 and 12 we give brief summaries and discussions of our results on geometry and polarisation, respectively.

2. Observations

The single-pulse observations used in our analysis below come from two programs carried out at the Arecibo Observatory over a long period of time. The older 430-MHz observations were carried out in 1973–74 with a single-channel polarimeter of 2.0-MHz bandwidth and 0.66-ms integration time, giving a nominal time resolution of about 1.1° longitude. The polarimetry scheme is described in Rankin, Campbell & Spangler (1975); no means was it then available to correct the Stokes parameters for the known cross-coupling in the feed, which could produce spurious circular polarisation at a typical level of about 10% of the linear.[6]

The newer observations at 430 and 1414 MHz were made in a single observing session in October 1992. Pulsar 1929+10 was observed as often as possible as a polarisation calibrator, and full-sky tracks (multiple 'scans' comprising the full time that the pulsar was accessible to the Arecibo instrument, about two hours of total integration) were carried out at 430 MHz on the evenings of the 16th and the 26th and at 21 cm on the evening of the 23rd. These observations sampled the 40-MHz

[6] We now know (see Rankin, Rathnasree & Xilouris 1998) that the cross-coupling in the 430-MHz feed varies markedly across the 10-MHz bandwidth of the feed. Generally, it introduced spurious circular at a level of some 10% of the linear. However, it was just for pulsars such as 1929+10 which have the smallest dispersions (and consequently the largest-scale scintillation structure) that the feed could most distort the polarisation. If most of the received power was in a single scintile near 435 MHz, the spurious circular could be as high as 35% of L.

correlator, which continuously 'dumped' the ACFs and CCFs of the right- and left-hand channel voltages at 400 μs intervals, which were then subsequently sorted out in time modulo the phase of the pulsar in the on-line computer.[7] The higher frequency observations used a total bandwidth of 20 MHz and the lower 10 MHz. The retention of 32 lags in both cases reduced dispersion delay across the bandpass to negligible levels. The resolution was then essentially the correlator dump time or 0.64°.

Individual-pulse observations were also carried out for pulsar 1929+10 at 1414 MHz on October 18th, using a special program to gate the 40-MHz correlator. The time resolution of these observations is a little smaller as the dump time was 306 μs or 0.49°. In all cases the measured correlation functions were 3-level-sampling corrected, calibrated, and Fourier transformed to produce raw Stokes parameters, which in turn were corrected for dispersion, Faraday rotation, instrumental delays, and all of the known feed imperfections. This procedure, we believe, has resulted in some of the highest signal-to-noise ratio (S/N) and accurately calibrated single-pulse polarimetry observations ever carried out. The details of the technique will be described in a forthcoming report (Rankin, Rathnasree & Xilouris 1998).

3. The main-pulse profile

In the polarimetry efforts at the Arecibo Observatory, we have learned to pay close attention to pulsar 1929+10. Dan Stinebring (Stinebring *et al* 1984a) first used this pulsar as a feed-coupling calibrator in 1981 because of its large and stable polarisation, and no pulsar within the telescope's view has been found since which approaches its usefulness as a polarisation calibrator. Therefore, during our October 1992 program, we observed 1929+10 on a number of days for as much as possible of the 2+ hours that the pulsar was in view. On a few of the days we were able to observe at 430 MHz (kindly thanking the United States Navy for several brief intervals free of gratuitous ship-borne radar interference), and on the remainder at 1400 MHz. All of these 'calibration' observations were made in the 'averaging mode'—that is, by accumulating the 32-lag ACFs and CCFs in 1024 phase bins across the pulsar period for typical integration times of 220 seconds. Given the pulsar's small DM, the dispersion sweep time was negligible compared to the 400 μs dump time of the correlator, so that the effective time resolution was essentially 1.8 milliperiods or 0.64°.

Apparently, our resolution was smaller than that of earlier measurements, because these new profiles reveal additional structure in the pulsar's average profile, both at 430 and 1414 MHz. It is hardly surprising that our resolution is better than that of the older work carried out with inferior techniques. However, both Phillips (1990) and Blaskiewicz *et al.* (1991) used the same correlator and polarimetry technique that we did. Therefore, they must have missed the new structure because the focus of their attention was on the overall, full period, polarisation-angle traverse.

These new observations are shown in Figure 1(a and b), and it is illuminating to compare them with those in Hankins & Rickett's figure 1(i), where we can see the

[7] The Arecibo 40-MHz correlator is described by Hagen (1987) and the observing software by Perillat (1988, 1992).

usual three components of 1929+10's triple profile. In the latter's figures at 430 MHz, the prominent components are II and III; whereas at 21 cm, I and II are most easily distinguished, and III is discernible merely as an inflection on the trailing edge. The profiles we obtained in Fig. 1 are clearly more complex. At 430 MHz (Fig. 1a), we can identify the usual three components as the primary peak (II), the secondary peak (III), and the second inflection on the leading edge (I). However, there are also two other identifiable features, both nearly symmetrical inflections on the leading and trailing edges of the profile, respectively. Note that all of these features can be discerned both in the total power (Stokes parameter I) and in the total linear polarisation L.

A similar situation can be seen in the 1414-MHz (Fig. 1b) profile. Here the usual three components are now readily apparent, but once again we also see marked inflections on the leading and trailing edges of the profile. Note that these new features can also be seen in the linear polarisation. Several earlier Arecibo polarimetry efforts at 21 cm (Stinebring *et al.* 1984a: figure 21; and Rankin *et al.* 1989: figures 1

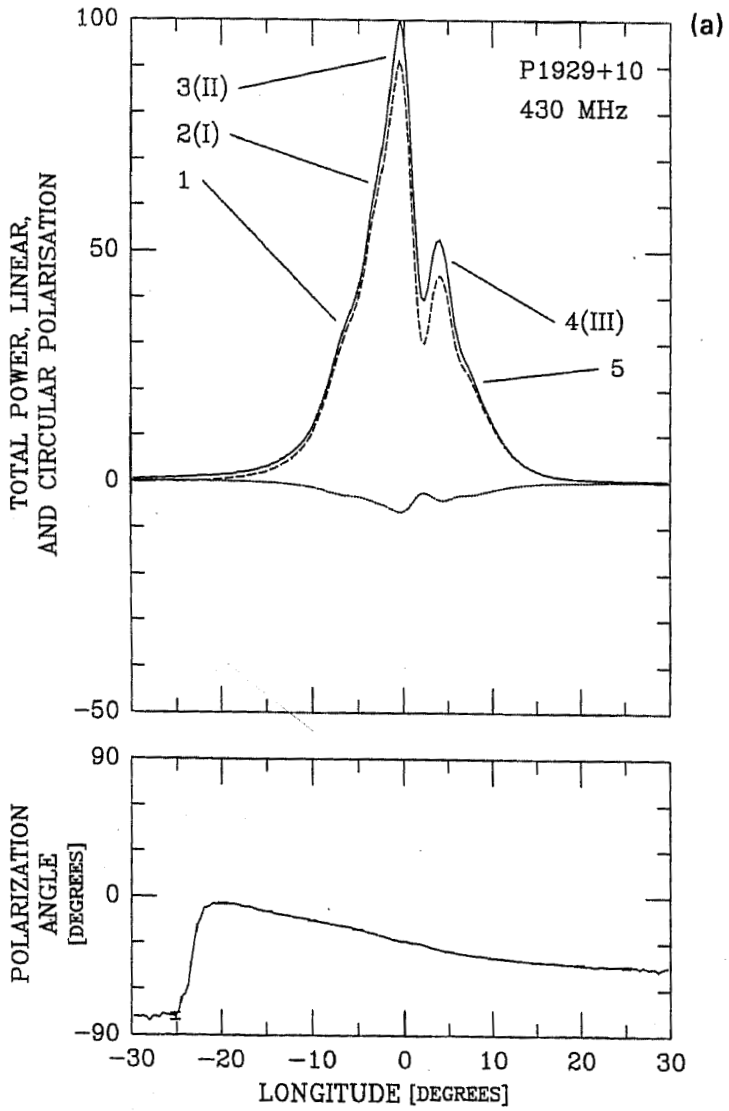

Figure 1. (*Continued*)

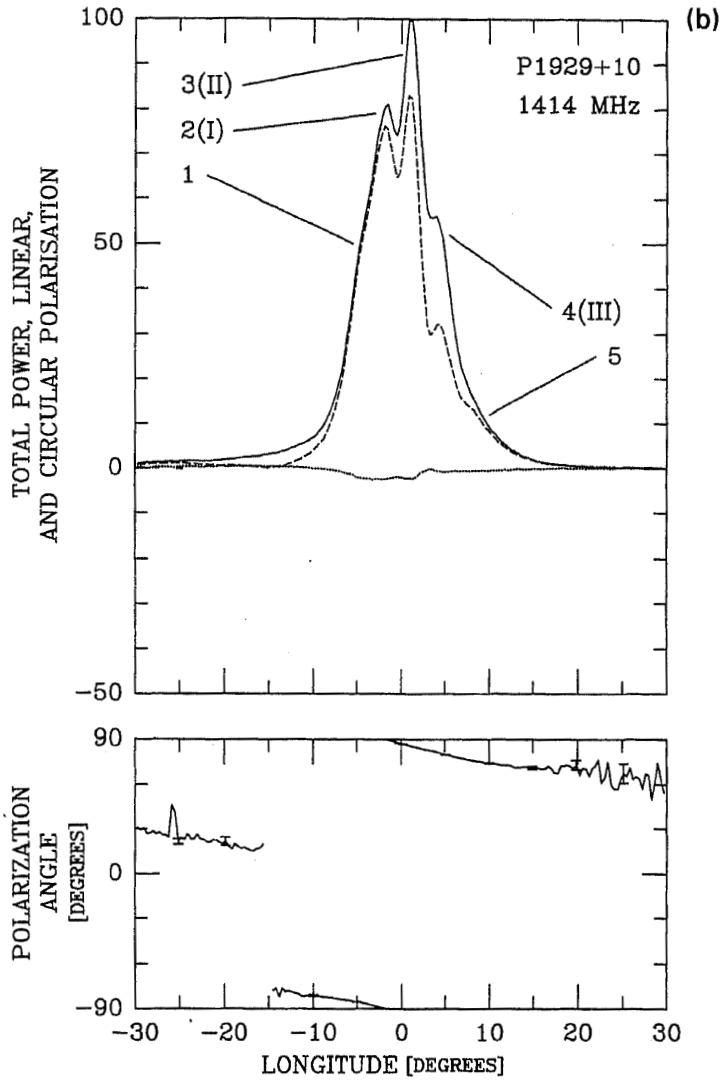

Figure 1(a & b). Average polarisation profiles for pulsar 1929+10 at (**a**) 430 MHz (12,197 pulses from 16th October 1992) and (**b**) 1414 MHz (21,703 pulses from 23rd October 1992). The topmost curve is the total power (Stokes parameter I); the next is the total linear polarisation ($L = \sqrt{(Q^2 + U^2)}$); the third curve is the circular polarisation (Stokes parameter V); and the bottom curve is the polarisation angle ($\chi = \frac{1}{2}\tan^{-1} U/Q$) with occasional 2-$\sigma$ error bars. These profiles have a true resolution s of 400 μs or about 0.64°. Error boxes ($\pm s \times \pm 2\ \sigma$) on the longitude axis near −25° have almost vanished into the widths of the plotted curves. The three major components are labelled as I-III: comps. II and III are most easily discernible at 430 MHz with comp. I visible as an inflection high on the leading edge of the profile, whereas at 1414 MHz all three components are readily distinguishable. Note, however, the additional pair of inflections on the extreme leading and trailing edges of the profiles. These features are denoted as comps. 1 and 5—and the foregoing ones, then, as comps. 2–4, respectively—throughout the text.

and 22) show these features much less clearly, although the claimed resolution was marginally better (342 and 386 μs, respectively, as opposed to the present 400 μs) than that here.[8]

[8] Apparently, earlier estimates of the dispersion 'smearing' and the effects of the integrator time constants were overly optimistic.

Kramer (1994) has also observed 1929+10 at 1400 MHz and then fitted a series of Gaussians to the profile. His tiny figure 13 does not permit close examination, but it is interesting to note that he required six Gaussian components to fit the profile, five of them in just the positions we have discussed above (and one additional to fit the long slow rise on the far leading edge of the profile). While it is not clear that a Gaussian is the correct functional form for a component, Kramer's careful fitting work certainly demonstrates that three components are an entirely inadequate description of this pulsar's profile. It is also worth noting that the added components are not so much small in amplitude, but simply so closely spaced that they are difficult to distinguish.

We also observed one sequence of 1414-MHz individual pulses during the same October 1992 program, and this observation has a slightly better resolution of 306 μs. The average profile comprised of these 2456 pulses is shown in Fig. 2(a), and we see that the same five profile features are present. One possible means of assessing the significance of the several profile features is that of constructing a histogram of the sample bins in which the individual-pulse maxima fell. This histogram is given in

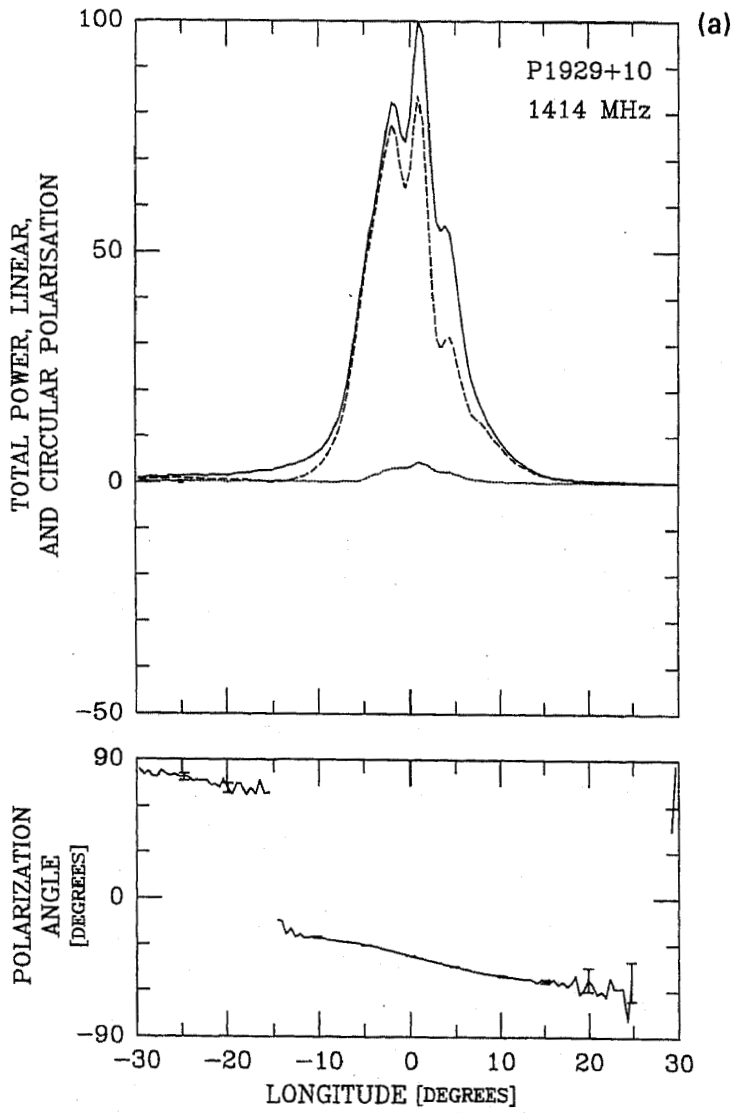

Figure 2. (*Continued*)

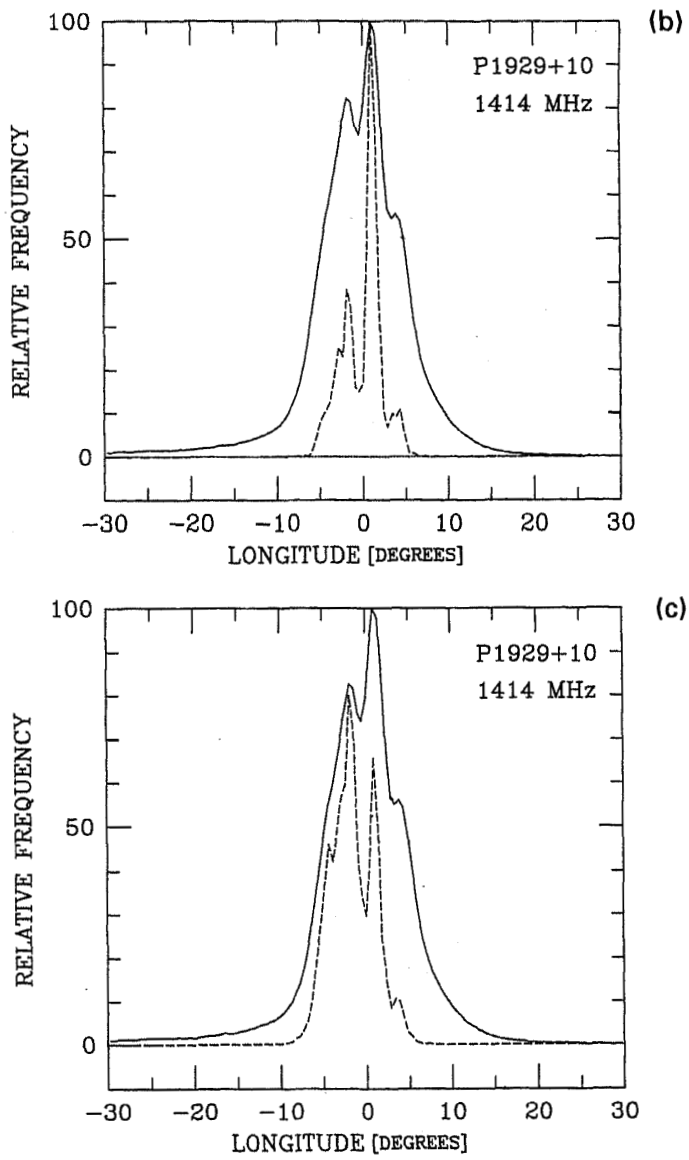

Figure 2(a–c). (**a**) Average 1414-MHz polarisation profile (solid line) comprised of 2456 individual pulses from the observation of 18th October 1992 as in Fig. 1. The resolution here is slightly better, 306 μs, than that in Fig. 1(b). (**b**) A histogram of the position of individual-pulse maxima using the same pulse sequence is shown as a dashed line; the average profile is also shown for reference. (**c**) Histogram of 'subpulse' peak positions calculated as in (**b**) (see text).

Fig. 2(b) (dashed line). The principal maximum of the histogram, of course, corresponds to comp. II and the lesser maxima to comps. I and III. Note, however, that there is one further feature at the beginning of the histogram (at $\sim -4°$ longitude) which seems to correspond to the earliest feature in the profiles, but nothing corresponding to the trailing feature in the profiles is really apparent.

Instead of looking just for the longitude of peak intensity, any number of additional peaks can be delineated in a single pulse and then checked to see if they represented a 'subpulse' of significant intensity (i.e., exceeding 1% or so) compared to the maximum subpulse intensity. The amplitude of these 'subpulse' maxima were then accumulated according to their longitude of occurrence and their resulting total amplitudes plotted as a function of longitude. The resulting Fig. 2(c) (dashed line) is a

distribution which closely resembles the overall structure of 1929+10's average profile. Again, four features are discernible, those corresponding to the usual three components and the leading-edge feature.

Let us leave this section, then, by simply restating its conclusion: well resolved, deep profiles of the 1929+10 MP at both 430 and 1420 MHz appear to have five—not three—features. Therefore, there is a case to be made that 1929+10 is another example of a five-component (M) pulsar. The usual components of its ostensible triple profile I, II and III then correspond to 2, 3 and 4 of the five-componented one—and we shall thus use Indian numerals 1–5 in what follows to enumerate them (Fig. 1 shows this correspondence schematically). The new pair of features is subtle, and so we should not rush to any immediate conclusions. Let us then leave the question of their significance in abeyance for the moment and examine other evidence before attempting to make any interpretation.

4. Full-period, average polarimetry

We have also carried out full-period, average polarisation observations in the manner reported previously by both Phillips (1990) and Blaskiewicz *et al.* (1991), and some of our observations are depicted in Fig. 3. Because pulsar 1929+10 was so important for overall polarimeter calibration, some extended observations were made on this pulsar, which resulted in multiple days of exceptionally sensitive and accurately calibrated data. Few pulsars have ever been observed with such remarkable sensitivity. The 430-MHz profile in Fig. 3(a) represents the strongest 12 of 27 220-s (986-pulse) scans, weighted according to their respective S/N ratios, and achieves a peak intensity to *rms* off-pulse noise level of fully 40 db. And, as we now know, pulsar 1929+10 is particularly interesting in this regard because it exhibits emission over most—if not all—of its rotation cycle. The MP peak in Fig. 3(a) is constrained to fall at about 0° longitude in the center of each plot, so that the other major emission features, the IP and PC, can be found at about −173° and +110°, respectively, in Fig. 3(a).[9]

There are, however, a number of other features in the 430 MHz profile: a break on the extreme leading edge and a 'component' on the trailing edge of the MP, and two other 'components' immediately following the IP. Each of these features is clearly seen in Phillips' figure 2 and less so in both Hankins & Rickett's (1986) figure 3 and Blaskiewicz *et al.*'s figure 22. What is new in Fig. 3(a) are the 'notches' in the leading part of the PC. These features can also be seen clearly in our 430-MHz observations on other days, and also are barely apparent in the figures of Hankins & Rickett and Blaskiewicz *et al.* referred to above.[10] To our knowledge, no such features have been described in the literature, and thus these 'notches' apparently represent a new

[9] All of the profiles in this paper are aligned to that the total power divides equally about 0° longitude.

[10] Interestingly, these 'notches' are not apparent in Phillips' figure, and it is interesting to try to understand why not, as both observations were made with the Arecibo 40-MHz correlator using the same bandwidth and dump time. Comparing Phillips' 430-MHz MP profile (see his Fig. 1) with ours or with Blaskiewicz *et al.*'s, it appears that his resolution was seriously compromised, either through observational errors or by smoothing which he did not report. We should bear this fault in mind in assessing his arguments and conclusions below.

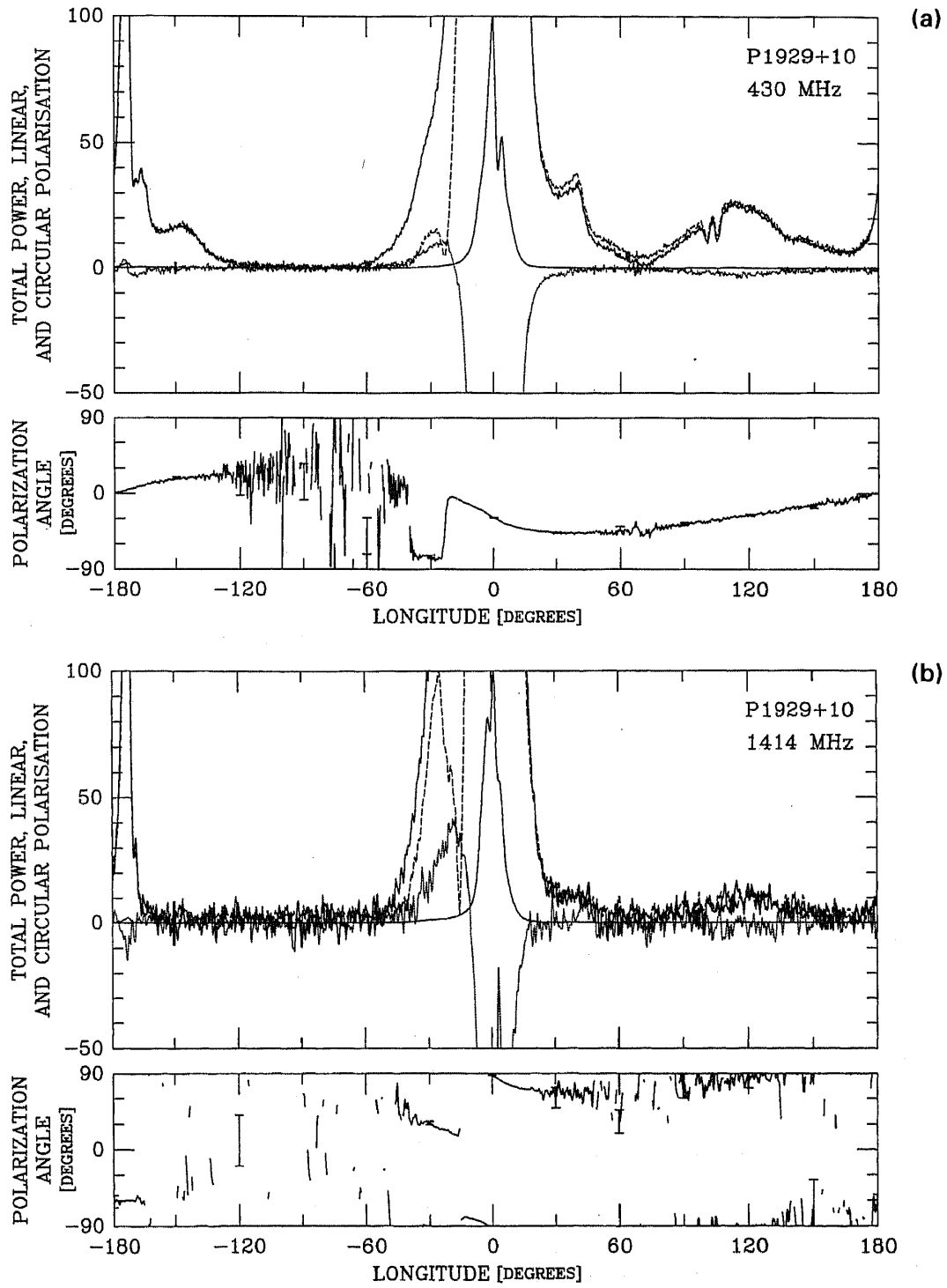

Figure 3(a & b). Full-period, average polarimetry of pulsar 1929+10 at (**a**) 430 MHz and (**b**) 1414 MHz as in Fig. 1. In each figure the total power is plotted first at full scale and then at an expanded scale of 100, so that only features below 1 per cent of the MP amplitude are now visible. The linear and circular polarisation are then plotted at the expanded scale and the PA as in the foregoing figures.

observational aspect of pulsar emission. While the PC component is also discernible in the 21-cm profile of Fig. 3(b), the poorer S/N ratio leaves open the question of whether the 'notches' persist at the higher frequency.

The polarisation of 1929+10's emission is also very interesting. The fractional linear polarisation is very large, essentially complete at every emitting longitude *except* under the MP. How paradoxical it is that the MP, long noted for its large linear polarisation, is the principal region of longitude at which less than complete linear emission is found within the profile! The lowest polarisation is associated with the polarisation mode change on the extreme leading edge of the MP, between about −50 and −60° longitude, where the emission is rather weak.[11] Otherwise, from the trailing edge of the MP throughout the full extent of the PC and IP, the emission is virtually fully linearly polarised.

Indeed, over a certain range of longitude the linear polarisation L is running somewhat in excess of 100%, despite the correction made to it for statistical polarisation.[12] In other longitude intervals (both where there is little power, such as the IP trailing edge, and where the intensity is high, on the trailing edge of MP comp. 4) the fractional linear polarisation, while large, does not exceed 100%. We found that this phenomenon persisted in our 430-MHz observations from other days (and it can just be discerned—with a magnifying glass—in Phillips' figure 1.[13]), and we have failed to conceive how its peculiar character might be understood on instrumental grounds.

We have begun to suspect that the excess linear polarisation is associated with the 'pedestal' of 'baseline' emission which Perry & Lyne (1985) detected in 1929+10 at nearly the same frequency. The zero levels for all of the Stokes parameters were taken in the lowest part of the 'noise baseline' between about −86 and −82° longitude—that is, in just the region in which Perry & Lyne were able to detect the continuous emission.[14]

---

[11] It also appears that there are minor secular variations in the details of the pulsar's polarisation, which are particularly apparent in the depolarised region preceding the MP. Note also that the circular polarisation, which is usually negative (rh), is slightly positive (lh) in Fig. 2(a).

[12] If we define the signal-to-noise ratio S/N as $L/\sigma_{\text{on-pulse}}$, the correction we used was $L_{\text{cor}} = L_{\text{raw}}\,[1 - 0.5/(S/N)^2]$, for $S/N > 1.25$, and $L_{\text{cor}} = L_{\text{raw}} - \sqrt{(\pi/2)}\,\sigma_{\text{on-pulse}}$ for $S/N \leq 1.25$. The referee of another paper kindly pointed out that the statistical polarisation correction which one of us had been using for many years was wrong. In most cases, the effect of this error was trivial (and, indeed, though Fig. 3(a) has now been plotted with the correct correction, it is indistinguishable from an improperly corrected earlier version). The referee pointed out, interestingly, that the statistics of the linear polarisation and (2×) its angle have the same behaviour as those of the fringe amplitude and its associated phase in interferometry, so that Moran's (1976) statistical development can be applied as well to polarimetry.

[13] Blaskiewicz *et al.* did not plot their observations in such a way that makes it possible to tell.

[14] Interestingly, in the presence of a linearly polarised 'pedestal', registered by a polarimeter which (like ours) correlates lh- and rh-circular channels to obtain the linear Stokes parameters, the 'baselining' of Q and U represent a shift of the Q,U origin away from the usual point of zero in-phase and quadrature correlation between the circularly polarised channels. If the 'pedestal' PA is constant in time (or really rotational phase of the pulsar), this shift will have no effect on the measured linear polarisation of the pulsar. However, if the linearly polarised 'pedestal' rotates with the source, the linear polarisation origin established by 'baselining' will not be fixed and will have an effect on the measured linear Stokes parameters.

One can readily calculate that for a constant intensity, but rotating source of linear polarisation L_0, the process of taking an instrumental origin at some rotational phase ϕ_0 causes it to appear as a fluctuating source of twice its amplitude, that is $L' = 2L_0|\sin(\phi - \phi_0)|$. Stokes parameter I for this same source, measured from an instrumental origin taken at the same point, would be zero because the power does not vary. Clearly, in this unusual case, L would exceed I.

The effect on our actual measured L and the PA is more complicated, because it depends upon how the 'pedestal' Q and U align with those of the pulsar emission. Clearly, any effect will be minimal when the pulsar is most intense and when half a rotation of the pulsar brings the 'pedestal' PA back to the same orientation as at the 'calibration point' imposed by 'baselining' Q and U. While all this *may* explain why L exceeds I above, it is difficult to be absolutely sure. A simple way to confirm this explanation would be to change the point at which the 'baselining' is carried out, but this is not possible because no change of 'calibration point' in the possible interval between about -120 and $-70°$ longitude makes a significant change in the alignment between the 'pedestal' PA and that of the pulsar. We will have more to say about this in Section 13 below.

It then remains to comment on the remarkable interval over which the polarisation angle is measurable. Only in the interval between about -120 and $-70°$ is it poorly defined, and even here it is hardly random—a smoothed average would seem to give a very reasonable continuation of the values on either side. Apparently, we have an unusual opportunity in this pulsar to study the PA traverse as a function of longitude and to interpret it in terms of the fundamental emission geometry of the pulsar. We shall turn to this analysis in Section 8 below.

Finally, we turn to the 1414-MHz profile in Fig. 3(b), and it is immediately clear that the S/N is poorer. Overall, the profile is simpler than its 430-MHz counterpart. The feature on the MP far leading edge is now stronger; whereas, the 430-MHz trailing edge 'components' of both the MP and IP have almost disappeared, and the PC is weaker, but still discernible. The linear polarisation of the MP trailing edge, the IP and the MP is still nearly complete, and the far leading edge of the MP still shows the least polarisation, with the prominent 'mode change' now shifted some 5° later in the profile. Greatly reduced in extent is the region over which the PA is defined, but it is still much larger than for most other pulsars.

5. Polarisation-mode structure of the MP emission

Let us now turn to the polarisation-mode structure of pulsar 1929+10's profile. To some extent we know from the outset that it must be 'simple', both because the aggregate polarisation remains high in the wake of whatever depolarisation processes are occurring and because the star's excellence as a polarisation standard requires that its polarisation be stable. Nonetheless, we have long known that two polarisation modes are active in the individual pulses over a broad range of MP longitude, and the evidence here is that these two modes are very nearly orthogonal [see Backer & Rankin (1980): figure 14; and Stinebring *et al.* (1984a): figures 22 and 23].

The lower panel of Fig. 4 shows the polarisation position angle of each longitude sample (falling above a 3-σ threshold) in the 1414-MHz observations of 18th October 1992. Secondary-mode activity is seen in the trailing portion of the MP profile, centered at $\approx 3°$ longitude. There is also a hint of secondary-mode activity at longitudes earlier than the leading component. It is clear from the figure that only rarely does the secondary mode dominate the primary one in this pulsar.

Using the model-angle method of polarisation-mode deconstruction (Rankin *et al.* 1988; Cordes, Rankin & Backer 1978), we can take the following representation of the single-vector model to define the respective primary and secondary-mode PA

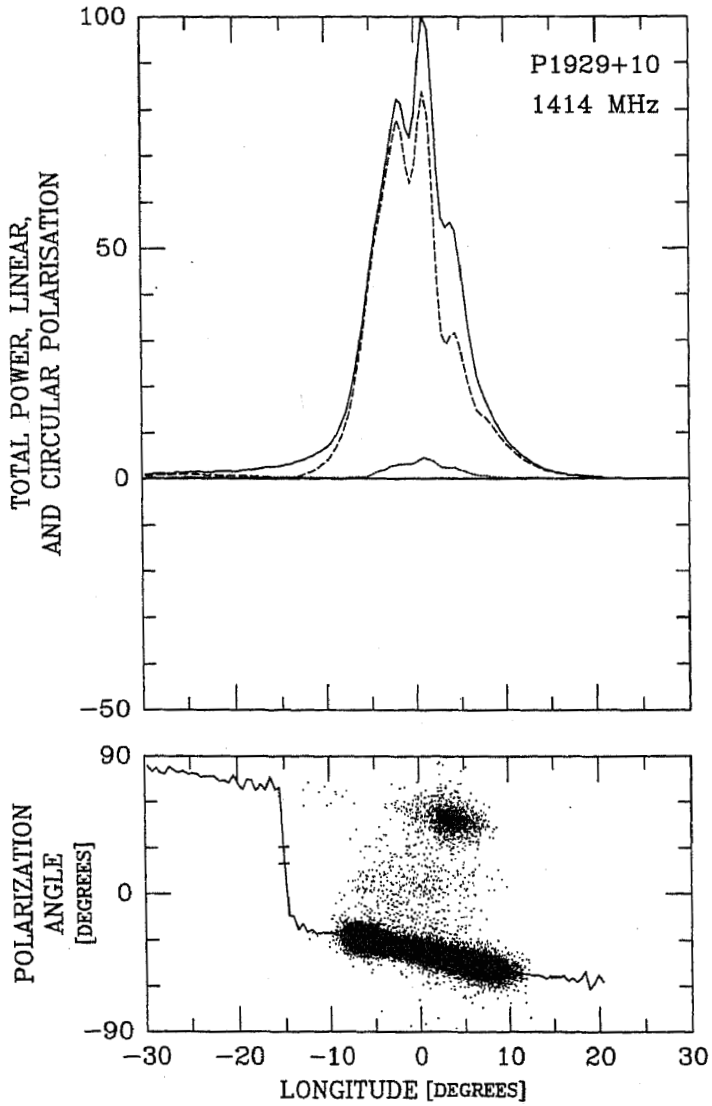

Figure 4. Polarisation-angle frequency for pulsar 1929+10 at 1414 MHz (from the single-pulse data in Fig. 2), showing the PA distribution with longitude for a sequence of 2456 pulses. The PA of each sample with L falling above a 3-σ threshold is plotted as a dot. The average PA is then superposed as a continuous curve with occasional 2-σ error bars. Note the 'over-exposed' primary polarisation mode track between about -10 and $+10°$ longitude. The secondary-mode emission is then strongest around $+4°$ longitude. The average PA then follows the PA of the weak secondary-mode emission on the extreme leading edge of the profile, and then 'jumps' to follow the primary-mode emission at about $-25°$ when it becomes dominant under the MP. Note the sharp minimum (close to zero) in the fractional linear polarisation, which coincides with the 'jump'; this is the only point in 1929+10's profile where the fractional linear drops below 50%.

traverses

$$\chi = \chi_0 + \tan^{-1} \frac{\sin(\phi - \phi_0)}{A - (A - 1/R)\cos(\phi - \phi_0)}, \tag{1}$$

where χ is the PA, ϕ the longitude, $R = |d\chi/d\phi|_{\max}$ the maximum PA sweep rate, and A a constant which can be computed from the total PA traverse χ_c between reference

longitudes $\pm\phi_c$ as

$$A = \frac{\sin\phi_c/\tan\frac{1}{2}\chi_c - \cos\phi_c/|R|}{1-\cos\phi_c}$$

and which is formally equal to $\sin\zeta/\tan\alpha$, where α and ζ are the angles that the magnetic axis and the sight line make with the rotation axis, respectively.

Turning now to the 1414-MHz observations shown above in Fig. 2 and taking the centre of the primary-mode polarisation traverse at about +4° longitude, where the PA is some −42°, R about $-1.4^{\circ}/^{\circ}$, and computing A from a total traverse χ_c of 30° at ±15° longitude, we proceed to construct the partial modal profiles. The individual-pulse samples were compared with a threshold—Stokes parameter $L \geq$ twice the off-pulse baseline noise level—and those samples falling below it relegated to a 'residual' profile. Those samples exceeding the threshold were then accumulated in the primary- or secondary-mode profiles depending upon whether the computed sample PA fell within ±45° of the model PA.

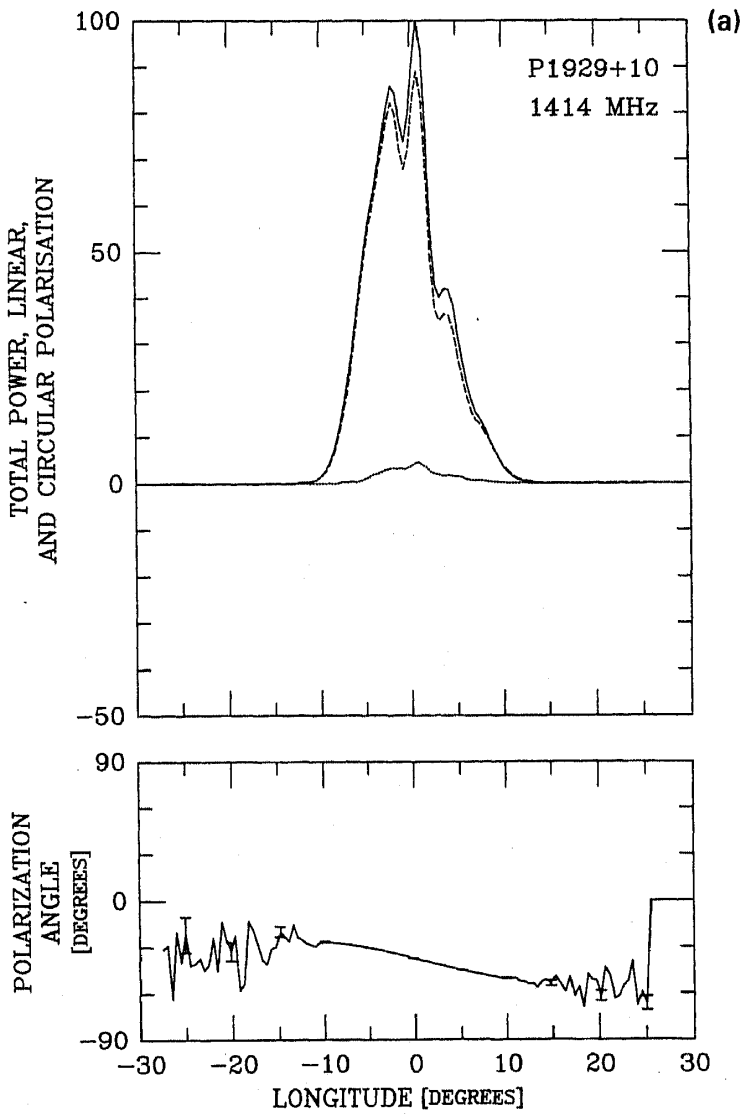

Figure 5. (*Continued*)

These three partial profiles are given in Fig. 5(a–c). The primary-mode profile (Fig. 5a) bears a strong resemblance to the total profile in Fig. 2 but is somewhat more highly polarised as expected. It is also missing its long slow rise and the relative intensity of comp. 4 is reduced. The secondary-mode profile (Fig. 5b) is more arresting: it consists of a single 'component' with a long 'bridge' of very weak emission preceding it, and, interestingly, it is not so highly polarised. Careful examination of the position of this feature reveals that it is coincident neither with MP comps. 3 nor 4, but rather falls between them, peaking near their common minimum; it follows comp. 3 by some 2.3° and precedes comp. 4 by about 0.8°. Reference to the residual profile (Fig. 5c) shows that a good deal of power did not meet the threshold, and most of this is secondary-mode power at longitudes before the modal PA 'jump' and primary-mode power thereafter. This latter profile represents, at 13%, a significant part of the total profile power, as compared to 6% for the secondary- and 81% for the primary-mode profiles, respectively.

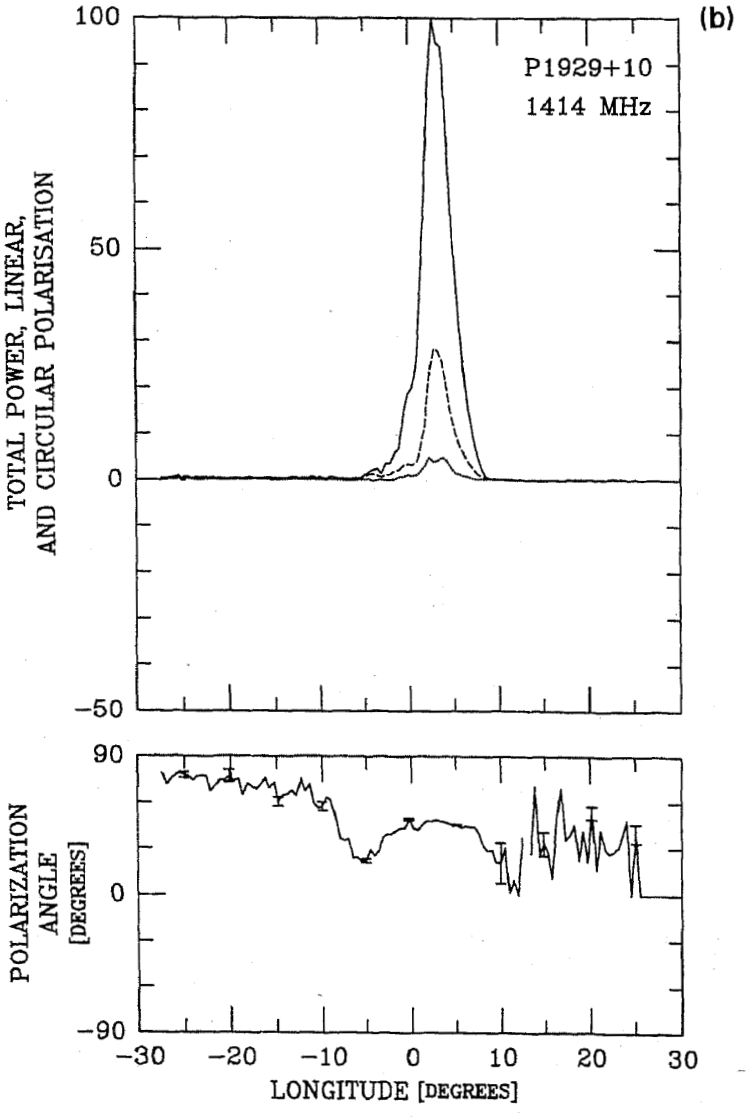

Figure 5. (*Continued*)

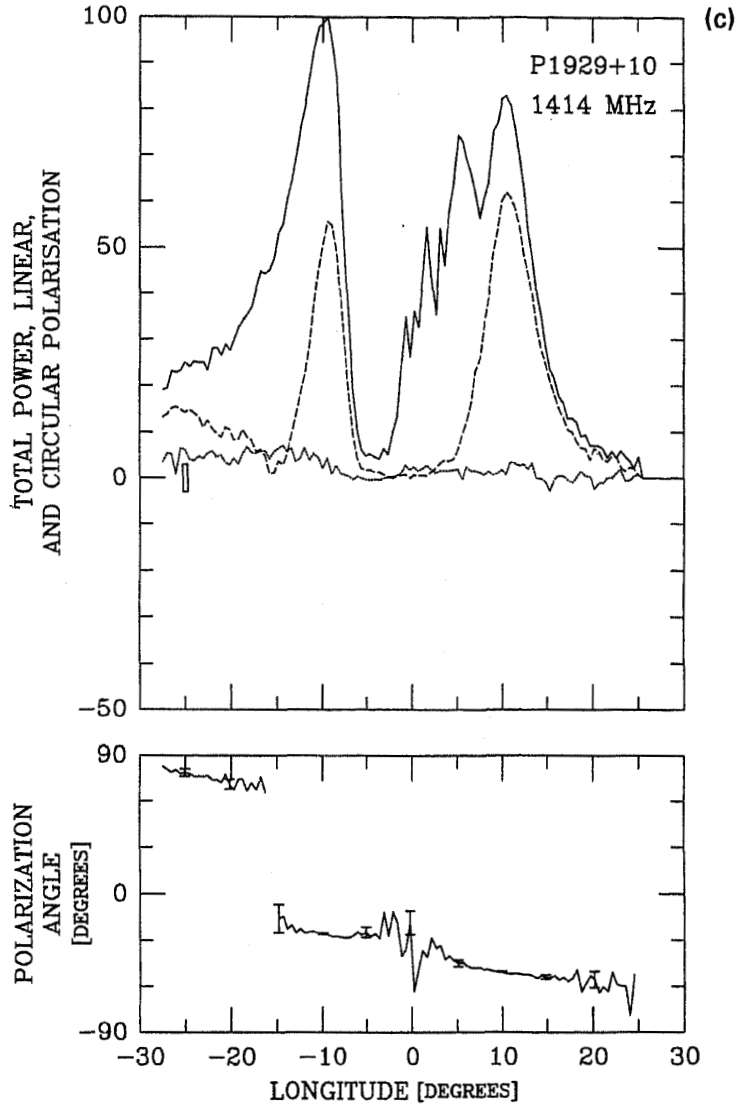

Figure 5(a–c). Partial, 'mode-separated' profiles for pulsar 1929+10 from the data at 1414-MHz as in Fig. 2. The first two panels aggregate the individual-pulse samples which exceeded the noise threshold and fell within ±45° of the primary- or secondary-mode model PA at a given longitude; whereas the third panel aggregates those samples which were too weak to meet the threshold (see text). The 100% scales of the three plots in this figure represent, respectively, 94.7%, 14.3%, and 5.7% of the total profile Fig. 2.

We have made a very similar decomposition using 430-MHz, single-pulse observations from December 24th, 1974. However, the results are less insightful because the higher average polarisation at this frequency results in a smaller fraction of secondary-mode-dominated samples. Such samples comprised only 3.6%, and the residuals only 2.7%, of the total profile power, respectively. Again, the primary-mode profile bears a strong resemblance to the total profile, but is relatively weaker and more highly polarized in the region between comps. 3 and 4. As at 21 cm, the secondary-mode profile consists of a long, very weak 'bridge' of emission followed by a single 'component', which is closely aligned with the minimum between comps. 3 and 4—following the former by 3.2° and leading the latter by 1.3°. Again, the secondary-mode profile is not very highly polarised, less than 20% at maximum.

6. Polarisation-mode structure of the MP emission, revisited

We already have discovered a good deal about the structure of 1929+10's profile: it is highly polarised (which implies that the primary mode must dominate the secondary mode by a substantial factor), both polarisation modes are active throughout the full extent of the MP, and these two modes have nearly orthogonal PAs. Let us then hypothesize that *all* depolarisation in pulsar 1929+10 results from the incoherent superposition of the two polarisation modes. This then implies that the two modes are themselves fully polarised, and, evidently, orthogonal. Under these favorable conditions,

$$I_{\text{primary (secondary)}} = \frac{I_{\text{total}} \pm L_{\text{total}}}{2}, \tag{2}$$

and we can reconstruct the modal profiles without requiring individual pulses which must meet a noise threshold.

The results of this procedure are depicted in Fig. 6(a and b) for the 430- and 1414-MHz observations of Fig. 1, respectively. Here we have plotted only the total power because, under our assumption, both modes are fully polarised, and thus $I = L$ for each. The primary mode is plotted with a dashed curve, and the secondary with a dotted one (plotted 10× and 5× for clarity). There is much to see in these figures.

First, the great preponderance of the power falls in the primary mode at both 430 and 1400 MHz, representing 94.1% and 89.5% at the two frequencies, respectively. Secondary-mode activity then divides into two regions, a weak one on the extreme leading edge of the profile and a stronger one which peaks near the intersection of comps. 3 and 4. The primary-mode profiles resemble the total profiles above, having three main (and perhaps five total) components. What is remarkable about the secondary-mode profiles is both their similar form and their utter lack of resemblance to the primary-mode forms. There is simply no primary-mode feature on the leading edge of the profile where the secondary-mode profile first peaks, and its second

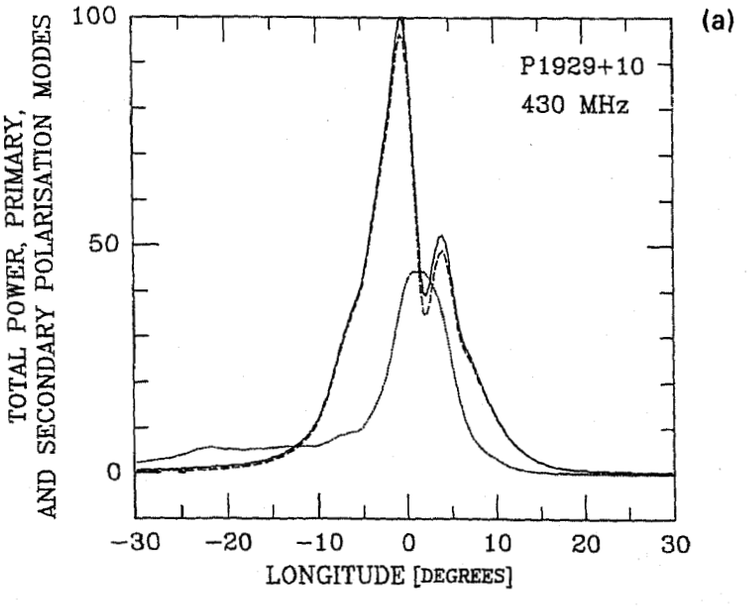

Figure 6. (*Continued*)

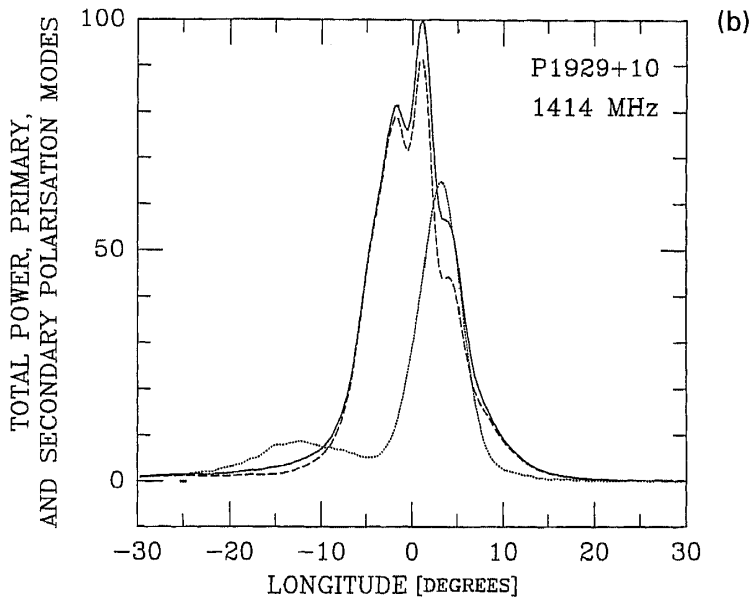

Figure 6(a & b). Empirical reconstruction of the partial polarisation-modal profiles at (**a**) 430 MHz, and (**b**) 1414 MHz, using the same observations as in Fig. 1. The primary mode is plotted with a dashed curve, and the secondary with a dotted one. The latter is also exaggerated for clarity by factors of 10 and 5, respectively.

'component' falls close to the minimum between MP comps. 3 and 4 and appears completely independent of them.[15]

This exceptionally clear decomposition of the polarisation modes in a highly polarised pulsar with a complex profile demands careful consideration. Yes, it does seem quite plausible in this case that *all* of the depolarisation results from the incoherent aggregation of power from the two orthogonal polarisation modes. However, we must critique this assumption as fully as possible. The fundamental difference in the form of the two profiles associated with the respective modes suggests that they are emitted in different places or propagate along different paths to radiate into our line of sight. We will consider these questions further below.

7. Modeling the modal depolarisation near the component 3/4 boundary

Let us now try to understand more about how these putative 'orthogonal' polarisation modes function to produce the depolarisation seen in pulsar 1929+10's pulse. Given the pulsar's overall nearly complete linear polarisation, the star provides an unusually good opportunity to study the character of what depolarisation there is in its profile. Reference to Fig. 4 illustrates this quite dramatically: at about longitude +4°, where the fractional linear polarisation reaches a local minimum, we see that there is a population of relatively strong single pulses which have PAs nearly orthogonal to that of the majority.

[15] Using this method we find that the secondary-mode peak follows comp. 3 by 2.1° and leads comp. 4 by 0.8° at 1414 MHz, which agrees quite well with the values in the foregoing section. At 430 MHz we find here that the feature trails comp. 3 by 2.0° and leads comp. 4 by 2.3°, placing it about 1.2° earlier than above.

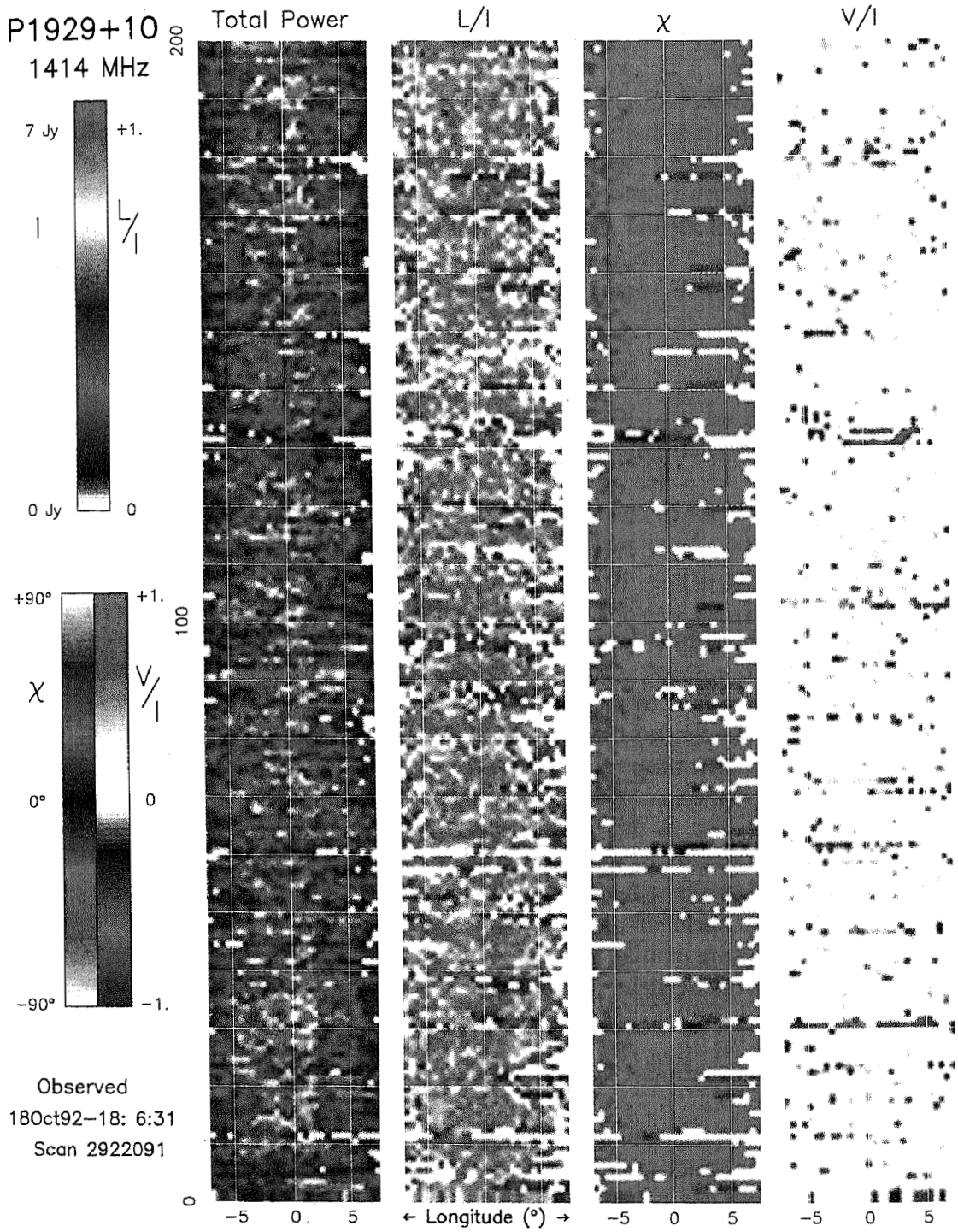

Figure 7. Single-pulse polarisation display of a 200-pulse sequence of the 1414-MHz observations in Fig. 2. The first column of the display gives the total intensity (Stokes parameter I), with the vertical axis representing pulse number and the horizontal axis pulse longitude (a range around the MP peak is shown here), colour-coded according to the left-hand scale of the top bar to the left of the figure. The second and third columns give the corresponding fractional linear polarisation ($L/I = \sqrt{Q^2 + U^2}/I$) and its angle ($\chi = 1/2 \tan^{-1} U/Q$), according to the right-hand scale of the top bar and the bottom-left bar, respectively. The last column gives the fractional circular polarisation (V/I), according to the bottom-right bar at the left edge of the figure.

We see this behaviour in more detail in Fig. 7, which colour codes the polarisation characteristics of a 200-pulse sequence at 1414 MHz. The time evolution of intensity (I) is displayed in the first column, the fractional linear polarisation (L/I) and its angle in the second and third columns, and the fractional circular polarisation (V/I) in the fourth. The intensities and angles in these panels are colour coded as shown in the colour bars at the left of the figure. The ordinate of each panel spans a small longitude range centered on the MP peak, and the abscissa marks off the entire sequence of consecutive pulses. The consistently high linear polarisation and shallow PA traverse from pulse to pulse are immediately striking. Note, however, that this usual behaviour is punctuated by pulses dominated by secondary-mode emission, which are unusually intense, much less linearly polarised, and carry the 'orthogonal' PA. The transitions from primary- to secondary-mode dominance are rapid, most of them lasting only for a single pulse. We see several prominent groups, however, in our 2456-pulse observation; a few clusters of two or three—in two cases, 5 and 9—in the sequence as well as some tendency for such SPM-dominated pulses to follow each other with a two or three-pulse separation.

Of course, one wonders if these strong, secondary-mode dominated 'subpulses' have any statistical regularity, and Deshpande (1997) has kindly provided an insightful analysis of the pulsar's fluctuation spectrum, which is shown in Fig. 8(a). There, one sees two significant features: one at 0.1795 cycles/period, or a P_3 of 5.57 periods, and a weaker peak at about 0.095 cycles/period, which ostensibly corresponds to a P_3 of some 11 periods—very nearly like the '6s and 12s' which

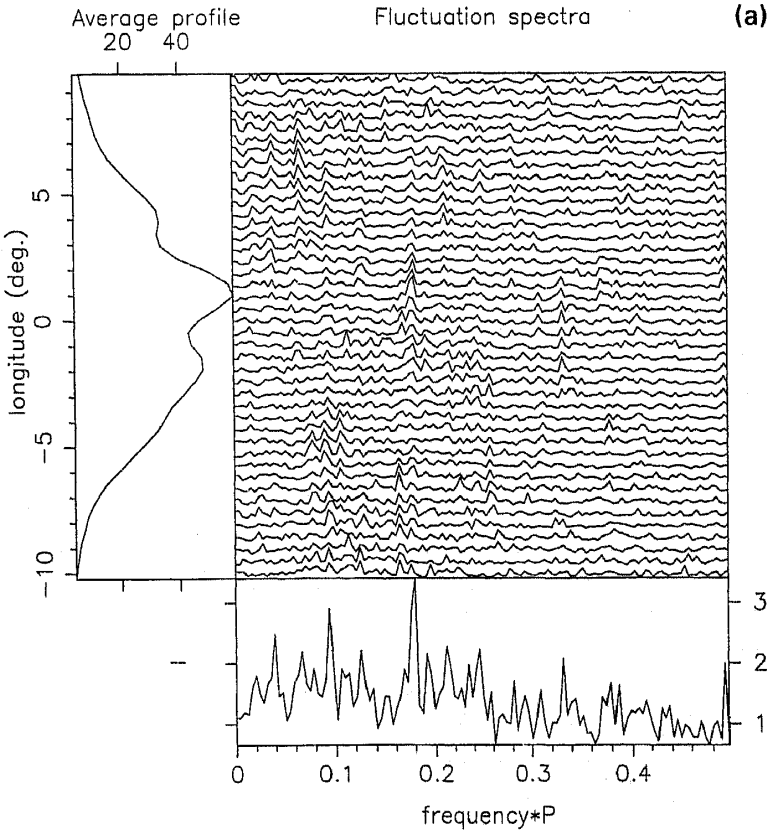

Figure 8. (*Continued*)

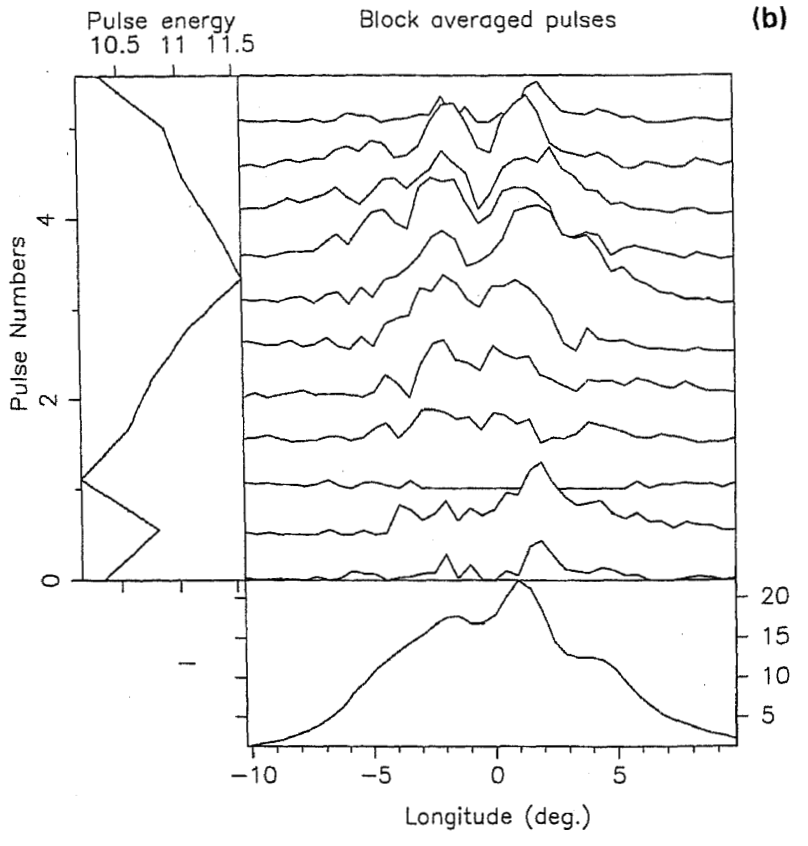

Figure 8(a & b). (**a**) Fluctuation spectra of the first 1000 pulses of the 1414-MHz observations depicted in Fig. 2. The longitude-resolved spectra are given in the body of the figure with a reference profile on the left and the average spectrum at the bottom. (**b**) Block-averaged difference profiles corresponding to the 5.57-period feature in (a). The constant base profile at the bottom has been removed from the difference profiles in the field, and their varying total energy is given at the left of the figure.

Backer pointed out in 1970. The strongest feature is most active near comp. 3, but can be traced over most of the width of the profile, except near comp. 4; whereas the latter is most active in the wings of the profile. Of the other minor features in the spectra, we see only one which is specifically active near the comp. 3/4 boundary—a weak feature near 3.33 cycles/period. This corresponds, of course, to a P_3 of 3, and indeed, several pairs of secondary-mode dominated subpulses can be seen in Fig. 7 which are just three pulses apart.

The strong 5.57-period feature seems to represent a pure, $\sim$10% amplitude modulation, and its effect is graphically depicted in Fig. 8(b). Note the way in which the various profile components stand out in these averages, particularly toward the peak of the modulation cycle. The behaviour of the weaker feature is more complicated: study shows that it is the alias of a modulation at 0.905 cycles/period, or a P_3 of just 1.1 periods. It appears to represent a phase modulation by a function whose width is considerably greater than that of the profile; therefore, it tends to modulate the amplitude of the edges of the profile selectively.

Further, it is useful to look at the average characteristics of the minority of rather intense single pulses, which are dominated by secondary-mode emission. Fig. 9 gives a pair of partial profiles corresponding to the total profile in Fig. 2(a),

which segregate those single pulses exhibiting secondary-mode emission at a level exceeding five standard deviations of the off-pulse noise. The primary-mode dominated partial profile in Fig. 9(a) is virtually identical to that in Fig. 5(a) (where a threshold of only 2σ was used), and this argues that virtually all of the secondary-mode dominated samples fall above the 5-σ level—we will see that this is more than true below.

The secondary-mode dominated partial profile in Fig. 9(b) dramatically illustrates just how curious this group of individual pulses is. Note first that the intensity scale of Fig. 9(b) is about 4/3 that of Fig. 9(a), leading to the conclusion that the power level at the comp. 3/4 boundary during intervals of secondary-mode dominance is about twice that during periods when the primary mode dominates. As expected the linear polarisation is low, and particularly so following the comp. 3/4 boundary. Comps. 3 and 4 are both unusually strong relative to the other features in the average profile, and all five components are discernible, most clearly in the total linear power. Finally,

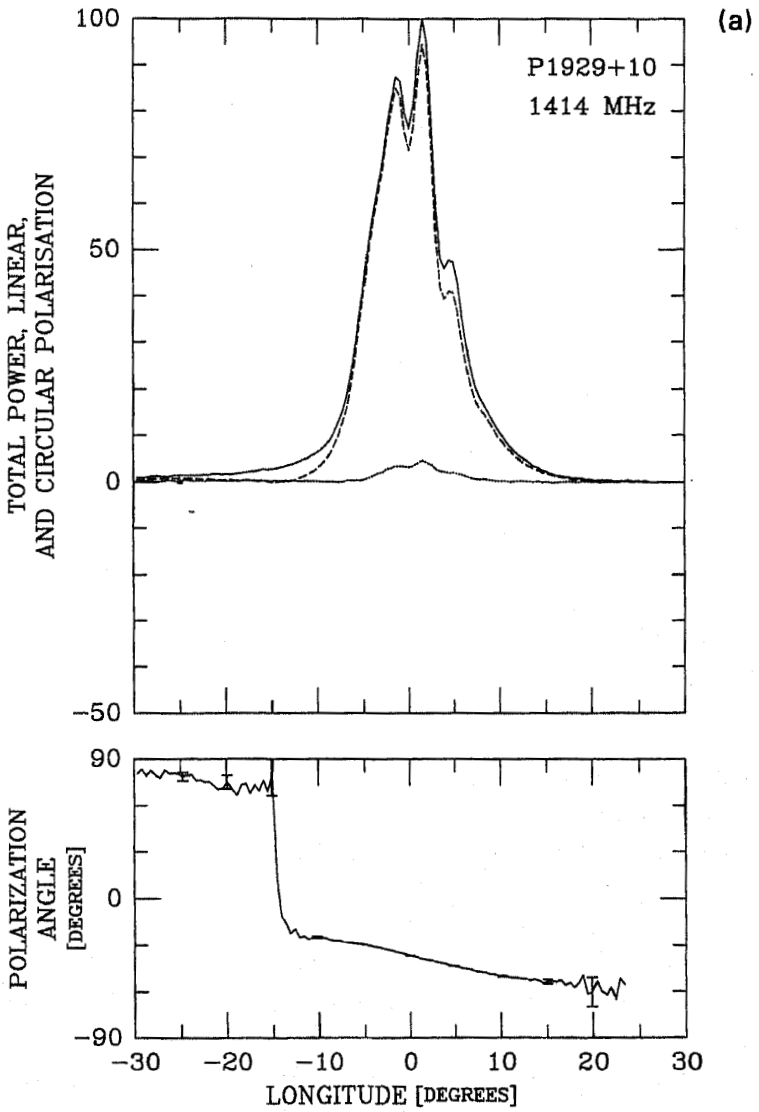

Figure 9. (*Continued*)

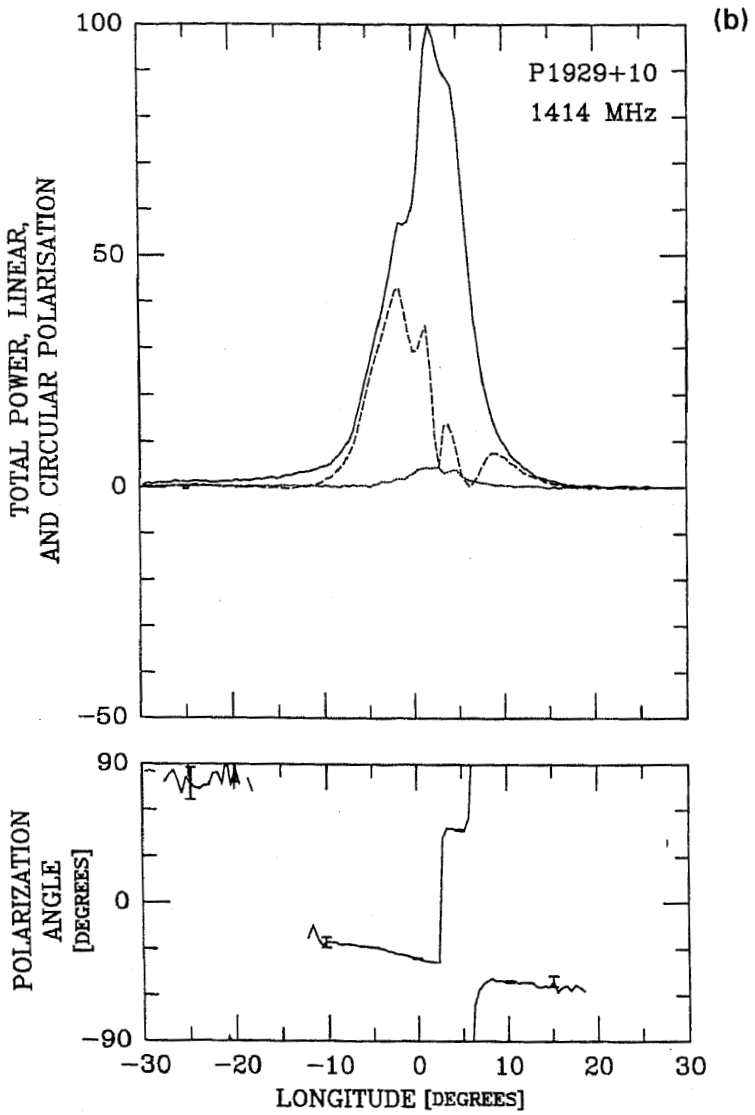

Figure 9(a & b). Pulse-by-pulse-separated modal average profiles of the 1414-MHz pulse sequence whose average is depicted in Fig. 2. (**a**) The average of those 2095 pulses which exhibited no secondary-mode emission at a level of 5 standard deviations in the off-pulse noise, and (**b**) the average of those 361 pulses which exhibited secondary-mode emission exceeding the foregoing criterion. The intensity scale of (**b**) is 1.34 times that of (**a**).

note the behaviour of the PA; at longitudes near comp. 4 the PA closely follows the secondary-mode PA track.

One further way of looking at the modal contributions to the total power and total linear polarisation is given in Fig. 10. Here we plot fractional linear L/I versus total power in a narrow, five-sample region near the comp. 3/4 boundary for each of the 2456 pulses in the 1414-MHz sequence, whose average is shown in Fig. 2(a). Those pulses with a PA near the primary-mode track are shown with 'x' symbols, and those with a PA near the secondary-mode track with an '*'. Here again we see that the primary-mode dominated emission is very highly polarised and rather weak compared to the secondary-mode dominated pulses. We see also that the former pulses are relatively steady in their intensity and that their distribution has some skew

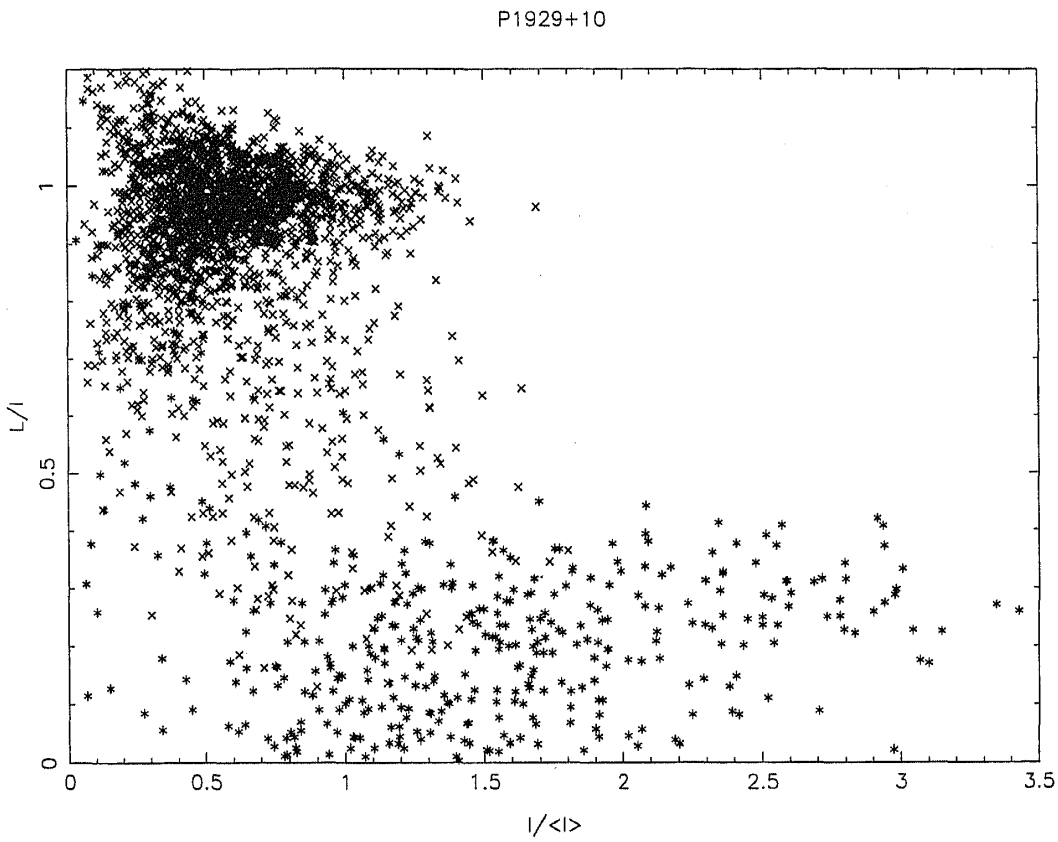

Figure 10. Scatter plot of fractional linear polarization L/I (corrected as in footnote 12) as a function of intensity $I/\langle I\rangle$ for the 2456-pulse sequence at 1414 MHz whose average is depicted in Fig. 2. The values here are computed in a narrow range of longitude (5 samples) centered on the boundary between comps. 3 and 4 at about $+4°$ (see Figs. 2 and 9). Pulses with a primary-mode PA in this region are indicated by crosses, while those with a secondary-mode PA have asterisk symbols. It is clear that the secondary-mode dominated samples in this region are both more intense and less linearly polarised than the primary-mode ones. The individual pulses typically have a S/N of about 30.

toward higher intensities.[16] By contrast, the secondary-mode dominated pulses exhibit a very broad intensity distribution with a mean at fully twice that of the primary and with rather little skew. This behaviour can also be seen in Manchester *et al.*'s (1975) figure 15.

It is tempting to try to model the depolarisation in this region near the comp. 3/4 boundary to explore the following question: can the depolarisation be understood as the result of incoherent superposition of two fully polarised and orthogonal modal contributions? Overall, the primary-mode emission from pulsar 1929+10 is so highly polarised that we may say it is essentially fully linearly polarised. The primary-mode dominated pulses in Fig. 10 give some indication of what the character of 'pure' primary-mode emission might be, but perhaps an even better indication comes from study of the near leading edge of the profile just below comp. 2, where the fractional linear polarisation reaches a local maximum of 96% at about 65% of the peak

[16] Note that the fractional polarisation of individual pulses can exceed 100% as long as the average in any intensity interval does not. We see, as expected, an escalating noise contribution to the uncertainty in L/I at lower intensity. The S/N ratio of these pulses is typically about 30.

intensity. The intensity distribution at this longitude (over a five-sample region, each longitude bin of which is first normalized by its mean) has a standard deviation of 0.58 and skewness of 1.66.

In our region of interest near the comp. 3/4 boundary, we can gauge the relative contributions of the two model modes on the basis of the total intensity and total linear polarisation; as in equation (2) the total intensity is the sum of two modal intensities, and the aggregate linear depolarisation is twice the intensity of the secondary mode. In this region the total intensity is about 54% of the peak intensity and the fractional linear polarisation is about 57%, making the secondary mode's relative contribution about 22% (to the primary's 78%) of the total intensity. The fraction of individual pulses with secondary-mode power at a level exceeding the 5-σ threshold in this region is some 15.4%.

We first attempted to model the two modal intensities I_p and I_s using χ^2-distributed random deviates χ^2_n and χ^2_m with different degrees of freedom n and m, respectively[17]—that is $I_p = 0.78\chi^2_n$, and $I_s = 0.22\chi^2_m$.[18] Using this model it is possible to get the fraction of secondary-mode dominated pulses about right; but no choice of the degrees of freedom comes close to correctly modeling the great disparity in the mean levels of the pulses identified as primary- and secondary-mode dominated (as in Fig. 10) or their greatly different aggregate polarisations.

A much more successful attempt retained the primary-mode model, but represented the secondary-mode emission as intense and intermittent. R is a uniform deviate in the interval 0 to 1; if R exceeds $0.22/a$, $I_s = 0$; otherwise $I_s = (a + bN)$, where N is a Gaussian deviate of zero mean and unity standard deviation and a and b are free parameters. The model gives a reasonable fit to the observed distributions for m, a, and b values of 9, 1.4 and 0.1, respectively. The modal ratio is almost exact; 376 pulses are found to be secondary-mode dominated (as opposed to 377 observed). The means of the two distributions are also almost exact, 0.81 and 2.04 for the primary and secondary, respectively (0.81 and 2.03 was observed). Less successful is the fractional linear polarisation given by the model, some 97% and 34%, respectively (as opposed to about 90% and virtually 0% observed). Neither does the model replicate the statistical properties of the primary- and secondary-mode dominated distributions very well. The worst discrepancy is the small standard deviation (normalized to the mean) of the model secondary-mode distribution, 0.15 (as opposed to 0.50 observed); the primary is closer, 0.53 (0.47 observed). The skewness of the model distributions is also greater than observed, 1.8 and 0.7 for the primary- and secondary-mode dominated distributions (as opposed to 0.7 and 0.4 observed), respectively.

These problems, notwithstanding, we believe that this modeling provides rather strong support for the proposition that the depolarisation in pulsar 1929+10 can be understood in terms of incoherent mixing of two orthogonal, completely linearly polarised modes. Theory cannot yet begin to tell us what manner of intensity statistics

[17] Backer (1971) was the first person, to our knowledge, to find that single-pulse intensity distributions were often well fitted by χ^2 distributions of a few degrees of freedom.

[18] The random deviates were generated using a modification of the GAMDEV routine in *Numerical Recipes* (Press *et al.* 1986). For small degrees of freedom, Gaussian deviates may be used to generate the χ^2-distributed random deviate as in ¶26.4.2 of Abramowitz & Stegun (1965); for larger degrees of freedom, the deviates can be computed from the incomplete gamma function as in ¶26.4.19 of the above work.

these parent distributions should have, and, lacking such guidance, any choices we make for the forms of these distributions will be somewhat *ad hoc*. Using distributions which are merely well motivated on the basis of the observations, we have come reasonably close to modeling the depolarisation accurately. It seems pointless to search for other *ad hoc* distributions which model the observations better or even perfectly. Our question has been addressed: mixing of two fully polarised modes does account quantitatively—and reasonably accurately—for the depolarisation in the comp. 3/4-boundary region of pulsar 1929+10.

Let us just emphasize one further point: both the primary and secondary-mode emission from this pulsar is quite steady. We found that the primary mode was fitted best by a χ^2 deviate with 9 degrees of freedom, implying that its standard deviation is only about 1/3 its mean value. Similarly, the most successful secondary-mode model was one which is quite uniform in amplitude, but intermittent in time. The intensity fluctuations in 1929+10 then stem very largely from the intermittency of the secondary-mode emission. Why the secondary mode should have this interesting and noteworthy characteristic is, at present, a matter of speculation.

8. What is the significance of pulsar 1929+10's remarkable PA traverse?

We now return to the question of pulsar 1929+10's emission geometry. As mentioned above several different groups of investigators have been lured by the unprecedentedly large interval over which the PA of this pulsar is measurable and have attempted to interpret the traverse in terms of the single-vector model. These results are summarized in Table 1, and it is clear that nearly every attempt—except Lyne & Manchester's (1988)—has resulted in values of the magnetic latitude around 30° and values of the MP sight-line impact angle around 20°—and some of the fits yield values with considerable precision.

None of this is immediately suspect; 1929+10 has a *very* shallow PA traverse associated with its MP, which would seem to indicate that β is comparable to α whatever its value. One might object that the pulsar has a rather complex MP profile for this putative geometry, but this doubt is hard to carry forward quantitatively. It is only when one begins to work out the implications of the IP geometry that serious contradictions begin to emerge. Narayan & Vivekanand (1982) viewed the pulsar as a two-pole interpulsar and were then forced to conclude that the IP impact angle must be some 87°! As this was the era when latitudinally extended emission beams were in vogue (Jones 1980), this geometry, although awkward, could not be dismissed out of hand. Lyne & Manchester's (1988) values seem to be the least well determined, but, being so much smaller, could be squared less awkwardly with a single-pole model for the IP, having an impact angle of 'only' 37.5°.

Phillips (1990) then provided unprecedentedly accurate values for α and $\beta_{\rm MP}$. In that his values are fully twice as large as LM's, $\beta_{\rm IP}$ must now lie between 70 and 90°, no matter whether we have a one- or two-pole interpulsar. This circumstance neatly points the question about the interpulse geometry. The vogue for latitudinally elongated beams had faded by the time that Phillips was writing, but, heedless, he opts in his figure 4 for a single-pole geometry in which the IP emission region lies fully 80 to 90° from the magnetic pole. Given that 1929+10's IP has a half-power width of hardly 5°, this now seems utterly preposterous.

Nevertheless, it is difficult to see how to reconcile this dilemma. A possible hint comes from the work of Blaskiewicz *et al.* (1991), who also obtain exacting values of α and $\beta_{\rm MP}$ (now based on a relativistic model of the PA traverse). They note obscurely that the inflection point of the pulsar's PA traverse lies not near the MP peak, but on the extreme leading edge of the profile. Given that this completely confounds their line of interpretation, they raise the possibility of 'nondipolar components' in the pulsar's magnetic field configuration.

In order to explore these questions further, we also carried out least-squares fits to the PA traverse of our 430-MHz observations [on 1992 October 16th (Fig. 3a) and October 29 (not shown)] using the single-vector model (e.g., Manchester & Taylor 1977; equation 10–24). The secondary-mode 'flip' at about $-25°$ was 'rectified' by adding 90°, and the transition region following it unweighted. We then considered how best to weight the rest of the values in the traverse. In principle, the errors in the PA are about $\sigma_{\rm on\text{-}pulse}/L$, and thus vary from 10^{-4} radians near the pulse peak to unity in the noise baseline. When the fitting was carried out using these weights, χ^2 was entirely dominated by the MP region; numerically the fit was quite unstable, and the remainder of the traverse was fitted poorly. In order to limit the dominance of the MP region, a lower limit was placed on the size of the errors, first at 0.1°, then at 1.0°, and finally only regions where $I/I_{\rm peak} \leq 0.005$ were fitted.

Our fit to the 16th October observations is shown in Fig. 11, and it is clear that the dashed curve fits the PA values reasonably well. Indeed, the reduced χ^2 is only about

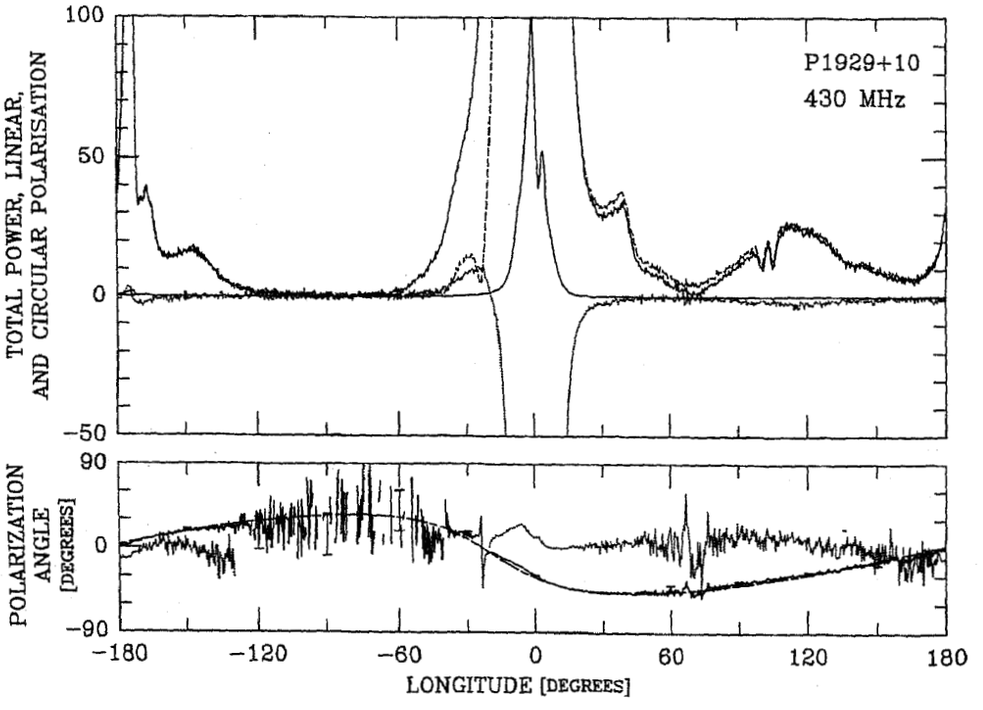

Figure 11. Least-squares fit (dashed curve) to the polarisation PA traverse in Fig. 3(a). A dotted curve shows the residuals to the fit (×5). The polarisation mode change on the MP leading edge has been rectified by a 90° rotation and the transition region following it unweighted. Then all points with intensities greater than 0.5% of the peak intensity were also unweighted (see text). Note the poor fit in the MP and IP regions. Note also that the inflection point of the fitted curve falls at about $-18°$ longitude.

3 when regions around the MP and IP where $I/I_{\rm peak} \geq 0.005$ are unweighted. The fitted values of α and $\beta_{\rm MP}$ resulting from the two day's observations are identical within their errors at $31.06° \pm 0.06°$ and $20.04° \pm 0.08°$, respectively.

We note, however, that the fit is quite poor just in those regions wherein we might expect the PA to be best determined—that is, under the MP and IP. (The dotted curve shows the residuals to the fitted data, exaggerated by a factor of 5 for clarity.) Most damning, though, is the circumstance that the inflection point of the fitted curve—which is associated according to the single-vector model with the longitude of the magnetic axis—lies some $-18.01° \pm 0.08°$ before the MP peak. These circumstances tend to undermine the strength of the geometric interpretations made on the basis of the single-vector model, and thus the values of α and $\beta_{\rm MP}$ resulting from any such fit are of uncertain significance.

Our work confirms the fitted values of Phillips (1990) and of Blaskiewicz *et al.* (1991), but this is all. Phillips, mysteriously, finds that the single-vector model fits his observations satisfactorily, and his figures seem to bear this out. He does not mention how he weights his PA data and passes over the significance of the offset inflection point with barely a mention. It is clear, however, in the excellent work of Blaskiewicz *et al.* that the fits are poor, and they both notice the position of the inflection point and regard it as a major issue.

This said, the question still nags as to why pulsar 1929+10's PA traverse should be so utterly misleading as regards its overall emission geometry.

9. Displaced modal emission and the conal geometry of the main pulse

With all of the foregoing discussion in mind, we come back to the question of pulsar 1929+10's conal emission geometry. Of prime importance is the question of whether this pulsar is a one- or two-pole interpulsar. Given the unusually large interval over which the PA is measurable, we might have expected that analysis of its PA traverse would at least settle this matter definitively. However, as we have seen in the foregoing section, the single-vector model fits the PA traverse poorly; its inflection point falls at a point far from what would appear to be the magnetic axis, and there is adequate reason to suspect that the PA traverse has been distorted and delimited in some manner.

So, then, if the factors arguing that 1929+10 has a small α value and thus a single-pole interpulse geometry are compromised, we are left with an abundance of other evidence indicating the contrary—that is, that the pulsar has an equatorial, two-pole interpulse geometry and therefore an α value near 90°. Among these pieces of evidence are the narrow MP and IP profiles and the half-power widths (interpolated to 1 GHz) of the putative core components, the IP and MP comp. 3, both of which are close to that of the polar-cap diameter $2.45°/P^{\frac{1}{2}}$.

In Paper VI we came to expect that when we understand the basic emission geometry of a pulsar in terms of its magnetic latitude α and sight-line impact angle β, then the conal emission radii ρ would assume one of two values, $\rho_{\rm inner} = 4.33°/P^{\frac{1}{2}}$ or $\rho_{\rm outer} = 5.75°/P^{\frac{1}{2}}$. As discussed above, pulsar 1929+10 eluded all efforts in this study to understand its conal beam geometry in these terms. Let us now see whether the new observational and analytical evidence adduced in the foregoing sections can help to clarify this dilemma.

Proceeding now on the assumption that α is about 90° and that β is near 0° for this pulsar, the spherical beam geometry of Paper VI figure 2 and equation (2) (see also Gil 1981) reduces to $(1/4)\sin\psi = \sin(\rho/2)$, or, for small angles, to $\rho \sim \frac{1}{2}\psi$, where ψ is the outside half-power width of a conal component pair (interpolated to 1 GHz) and ρ is the conal beam radius, measured from the magnetic axis to the outside half-power point of the beam.

Turning first to the conal component pair comprised by components 2 and 4, their ψ value, scaled to 1 GHz, was given in Paper VI (Table 5) as 13.2°. This implies a ρ value which is much too small to associate the pair with an inner cone—and we now know that it is overestimated, because it does not take into account the existence of comps. 1 and 5 in the profile. However, the new pair of features on the extreme leading and trailing edges of the profiles—which we identified above as comps. 1 and 5—have a half-power, 1-GHz width of about 18°. Of course, it is difficult to estimate their outside half-power width accurately from the profiles, but Kramer (1994; see his Table 14, comps. 2 and 6) gives data from which a 1.42-GHz value of 17.1° can be computed, and this in turn can be reasonably extrapolated to 1 GHz using a spectral index of about −0.13, giving 17.9°. This value compares very favorably with the $\rho_{\rm inner} = 4.33°/P^{\frac{1}{2}}$ value of 9.1°. Therefore, it appears that we should interpret the conal pair comprised by comps. 1 and 5 as resulting from an inner conal beam.

We turn now to the pair of secondary-mode features seen most clearly in the 'mode-separated' profiles of Fig. 5. These curves are simply bimodal and, if we also interpret them as a conal component pair, we can measure their outside half-power widths quite accurately. Interpolating the 430- and 1414-MHz values to 1 GHz, we obtain a value of 24.5° ± 0.5°. Remarkably, this squares readily with the $\rho_{\rm outer}$ value of 12.1°.

The 1929+10 MP profile provides us with a surfeit of features, a core component and what appear to be not two, but three conal component pairs. The two with the largest dimensions, the secondary-mode pair in Fig. 5 and comps. 1 and 5 exhibit ρ values which are in agreement with the $\rho_{\rm inner}$ and $\rho_{\rm outer}$ values given in Paper VI. So, paradoxically, it is the narrowest, strongest pair comprised by comps. 2 and 4 which appear to be anomalous geometrically.

There have been several prior hints of conal component pairs with implied ρ dimensions smaller than that of an inner cone, but components 2 and 4 of pulsar 1929+10 represent the most revealing instance to date. The high frequency outriders of the core-single (S_t) pulsar B1914+13 has an implied ρ value of 5.3° (see Paper VI Table 4). Interestingly, both this latter value and comps. 2 and 4 of 1929+10 (using Kramer's 1.4-GHz data and scaling as above) are roughly consistent in implying a ρ dependence for this 'further-in' cone of about $\rho_{\rm further-in} \cong 2.5°/P^{\frac{1}{2}}$.

We also find widths which fall below the $\rho_{\rm inner}$ and $\rho_{\rm outer}$ tracks in the work of Gil *et al.* (1993) and Kramer *et al.* (1994). Both studies, while verifying the general double-conal structure of pulsar emission beams, encountered a very few cases of emission components with ρ values smaller than that of an inner cone. This can be seen in figures 1–3 of Gil *et al.* and figures 8–10 of Kramer *et al.* (although one cannot readily identify just which pulsars correspond to the points in question). Moreover, these in-lying values appear consistent with each other (and with our results above) in suggesting a third conal beam with a dimension of about $2.5°/P^{\frac{1}{2}}$.

10. What is pulsar 1929+10's emission geometry? or How can the single-vector model tell a lie?

Our study was motivated initially by the paradox of pulsar 1929+10's emission geometry. Virtually all efforts to interpret the star's PA traverse according to the single-vector model (SVM) result in small values of the MP α and β, indicating that it has a single-pole interpulse geometry; whereas lines of interpretation growing out of profile classification indicate that the MP α is about 90° and β about 0°, making it a two-pole interpulsar. In most cases the two techniques are quite compatible in their ramifications, but in 1929+10 their implications are fundamentally contradictory. There is no middle ground: it is *only* for emission geometries which are *either* closely aligned *or* nearly orthogonal that reasonable impact angles for *both* the MP and IP can be achieved. What can we learn from this situation?

In weighing the evidence, we conclude that the two-pole interpulse model is far more compatible with the totality of what is known about 1929+10's emission, both qualitatively and quantitatively. Quite simply, it permits us to view its MP and IP features on the same basis as the vast majority of other normal pulsars, in terms of an emission-beam geometry comprised of core and conal features with specific period- and frequency-dependent angular scales. What we are forced to abandon is the powerful and very general implications of the single-vector model. We do not do this lightly; it is unsettling, and if we cannot understand the PA traverse of a star in which it can be delineated over most of its rotation cycle, when can we?!

The crux of the issue is certainly this: why should 1929+10's PA traverse be so patently misleading when that of virtually all other pulsars is either not so or much less so? We do not know, but we have some ideas. 1929+10 is not unique in exhibiting a 'funny' PA traverse. The case of B1237+25, for instance, is well known; most workers have assumed that it represents a very small impact angle, though this has not been justified quantitatively. A further short list of slow pulsars could include Bs 0823+26, 1055−52, 1541+09, 1742−30, and 2002+31. Each of these stars exhibits a 'disrupted' PA traverse, which does not seem to be the result of changes in the dominant polarisation mode—and for each there is good indication that the impact angle is quite small (see Paper VI and the references therein). The most interesting parallel to 1929+10 is pulsar 1055−52, which also exhibits an exceedingly shallow PA traverse. The geometry of its MP components and IP seem compatible quantitatively with a two-pole, nearly orthogonal interpulse geometry, but there is no clear support for this in its shallow PA traverse.

We also take note of the fact that there are virtually no pulsars with a PA traverse simply indicative of an essentially zero impact angle (i.e., $|\beta/\rho| \leq 0.1$). Lyne & Manchester (1988) attributed this to 'intrinsic or instrumental smearing effects' (see their much discussed figure 12), and a study in progress by Mitra & Deshpande (1997) has encountered a similar under-representation. No doubt such pulsars will comprise only a handful, but where is even a single good example to be found?

We tend to the conclusion that most extremely shallow PA traverses are suspect. Given the highly ordered and smallish dimensions of virtually all normal pulsar beams (i.e., Paper VI), it will be quite difficult to generate such traverses, except when the magnetic latitude is small. Clearly, some such traverses are observed, and pulsar B0950+08 provides a good example with its well studied single-pole

interpulse geometry; quantitatively, its α, $\beta_{\rm MP}$, and $\beta_{\rm IP}$ seem fully compatible with the dimensions of an inner cone. Most cases of shallow PA rates, however—when $d\chi/d\phi$ is of the order of unity—should be approached with caution, particularly when their geometrical implications appear anomalous.

The single-vector model depends on a number of conditions, which, given its near universal applicability, must be very generally true of the pulsar magnetosphere:

- a dipolar magnetic field configuration, implying emission from well within the light cylinder,
- relativistic beaming at high γs, so that each emitter is associated with a particular longitude,
- a narrow radial depth to the emission, so that there is no differential abberation or retardation and no superposition of physically separated emission components, and
- essentially free-space propagation within the pulsar magnetosphere and its environs.

Given the orthogonal-mode emission, we might also add

- that the modes truly be orthogonal, so that their superposition does not generate PAs unrelated to those emitted.

In the context of these considerations,[19] let us examine several specific mechanisms by which 1929+10's PA traverse could be distorted:

Non-dipolar magnetic field: The discussion in Blaskiewitz *et al.*, notwithstanding, we find no more reason to expect non-dipolar effects in 1929+10 than in most other pulsars. The angular dimensions of its emission components appear to be quite consistent with the overall slow pulsar population, and no particular anomalies are apparent in the frequency evolution of its profile.

Low γ 'smearing': Pulsar radiation has generally been regarded as coming from particle bunches moving with high γ values. However, there is evidence that some emission—core emission, in particular—comes from much lower γ emitters. We find many instances among the general pulsar population where the PA traverse near the central core component is distorted. Pulsar 1237+25 provides a remarkable example of such distortion, and Ramachandran & Deshpande (1997) report promising initial efforts to model its traverse using a low γ core beam. We strongly suspect that low γ 'smearing' is responsible for smoothing the PA variations in a number of pulsars. It is difficult to see, however, just how this mechanism could be responsible for the overall shallow traverse in 1929+10's case.

Multiple emission sources: Several sources of emission at a particular longitude would certainly violate the underpinnings of the SVM, and a number of cases can be found where this seems to occur just from the mixing of core and conal emission. The nearly complete linear polarisation in 1929+10, however, argues strongly that its emission stems, at most longitudes, either from a single source or from several coherent ones.

Extended emission-region depth: Closely related to the foregoing is the possibility that the received radiation is emitted over a range of heights in the magnetosphere. We reiterate that the radiation from pulsars with an equatorial geometry may entail emission over an unusually large depth, because it is only for

[19] Here we have closely followed a discussion by Cordes (1997).

such stars that certain trailing equatorial field lines have a continuous range of heights with a tangent in the sightline direction.

'Pedestal' Emission: The 'pedestal' emission is peculiar to 1929+10, and we have tried very hard to see if it could be responsible for the observed PA distortion. This emission cannot be directly detected using single-dish polarimetry, but if it is highly polarised *and* its PA varies with the star's rotation, we can expect to have some occasional low level intervals where L exceeds I and certainly some concomitant distortion of the linear PA traverse. Whatever effect this 'pedestal' emission has on the overall PA traverse, however, it cannot have much effect on that part of it near the MP and IP. Therefore, it cannot explain either the poor fit of the SVM or the shallowness of the rate in these regions.

Nonetheless, at Arecibo, using multiplying polarimeters which correlate dual-circular channels, the modest excess of linear polarisation at certain longitudes in deep (particularly 430-MHz) profiles appears to be a repeatable phenomenon. Whatever the origin of the 'pedestal' emission, it is closely associated with the pulsar; it is "inside the light cylinder" on the basis of the scintillation arguments, and the pulsar's virtually complete linear polarisation argues that both the 'pedestal' and pulsed emission have the same origin. This seems to point to the unprecedented difficulty in this pulsar of establishing instrumental origins for Stokes parameters Q and U, which are free of the effects of highly polarised and rotationally varying 'pedestal' emission. Unfortunately, we have no independent means to confirm this.

Propagation Effects: We understand very little, thus far, about what sort of propagation effects there might be in the pulsar environment, but the ostensible displaced modal emission associated with the secondary-mode profile might well be such an effect, as the 5–10° advancement of this component pair (relative to the MP centre) is much larger than what can be produced by retardation and abberation. Indeed, the equatorial geometry which seems most appropriate for 1929+10—that is, with both the magnetic axis and the sightline lying close to the equator of the star—appears to be one in which propagation effects might be particularly important, both within the magnetosphere or even just outside it. Nonetheless, we are able to see no straightforward means of obtaining the flat PA trajectory which is observed.

Non-orthogonality of the polarisation modes: We see little evidence of non-orthogonality in the polarisation modes in 1929+10. This may be an issue in other pulsars, but does not seem to be very important here. The PA traverse seems to accurately follow one mode or the other as can be seen, for instance, in Fig. 4, and only in the narrowest longitude range do the two modes have comparable intensities. The only evidence we see, for a slight non-orthogonality, is the assymetry of intermediate PAs between the primary- and secondary-mode tracks in Fig. 4.

11. Summary and conclusions: Geometry

A number of new and long known circumstances are identified which affect the question of this pulsar's emission geometry.

- A pair of new components have been identified in the star's average profile, both at 430 and 1400 MHz [and there is good evidence that the profile is also quite complex at 4.75 GHz in the work of Kramer (1994)], which can be interpreted as an inner cone.

- A further pair of secondary-mode 'components' has been identified, which appears completely independent of the overall MP component structure, and which can be interpreted as an outer cone.
- Fits to the star's PA traverse at 430 and 1414 MHz using the single-vector model yield α and β values of spectacular accuracy, but the model does not fit the observations satisfactorily.
- We identify several different sources of PA-traverse distortion including the pulsar's unique 'pedestal' emission; several of these appear to be most relevant to pulsars with an equatorial emission geometry, and
- the very closeness of the pulsar may facilitate our observing deep structure in this star which will perhaps never be seen in other pulsars.

How are we to weight all of these circumstances?

Much has hung in 1929+10's case on the significance of the low level emission far from the MP and IP—which permits determining its PA over such a large interval of longitude in the first place. The pulsar is virtually unique in exhibiting this low level, pan-longitude emission, and it is only by virtue of its locality that we are privileged to detect it. Whatever the geometric significance of this emission, its very low level almost certainly makes it susceptible to distortion, instrumentally, by the 'pedestal' emission,[20] which is probably emitted by the same sources as the pulsed emission and whose PA probably varies with the rotation of the star—otherwise the incoherent addition of the pulsed and 'pedestal' emission would probably produce observable depolarisation. Any rotating, 'pedestal' contribution to the pulsed linear Stokes parameters Q and U will tend to flatten the PA traverse as they must pass through zero level in order to achieve their full range of PA.[21]

Whatever are the issues surrounding the 'pedestal' emission, it cannot have a strong effect on the PA traverse where the radiation is intense—that is, near the MP and IP. Thus, we are still left with the shallow PA traverses in these regions. We note that **a**) 1929+10 is not alone in exhibiting a 'distorted' PA traverse, **b**) that we have some evidence that such distortion occurs when the impact angle is small and/or when the magnetic latitude is close to orthogonal, and **c**) that a number of potential and observed circumstances might have the effect of distorting the PA traverse, even when the emission is relatively intense. Nonetheless, we have not been able to understand just which of these circumstances is responsible for the PA-traverse 'distortion' encountered here.

The primary line of argument inferring that pulsar 1929+10 has a small α value and thus a single-pole interpulse geometry is, in our judgement, thoroughly compromised. Therefore, we can explore whether its profile morphology is compatible with

[20] The measurement difficulty we are encountering here is jointly a property of the pulsar (it has a 'pedestal') and the polarimeter (two circularly polarised channels which are correlated to produce Stokes parameters Q and U). A polarimeter which correlated two linear channels would be blind to the 'pedestal' polarisation. As far as we are aware, all the deep studies of pulsar 1929+10's polarisation have been carried out using the Arecibo instrument, where all of the polarimeters have been of the dual circular type. It would be useful to study the pulsar using the other kind of polarimeter; however, it may be that the questions raised by 1929+10's 'pedestal' polarisation will only really be addressed by sensitive and well calibrated interferometric observations.

[21] Carrying the example in footnote 14 one step further, one can calculate the PA behaviour which would be associated with this constant intensity, rotating source of linear polarization, and the result is that with 'baselining' it ceases to give any intimation of rotating with the source.

the usual two-pole interpulse geometry—that is, $\alpha \approx 90°$ and $\beta \approx 0°$. We cannot have it both ways. Now we are able to identify pairs of conal components which have the expected dimensions of both inner and outer cones; the new comps. 1 and 5 have almost exactly the interpolated, 1-GHz, outside half-power width that would be expected for an inner cone—that is, twice $\rho_{\rm inner} = 4.33°/P^{\frac{1}{2}}$ or 18.2° as opposed to a measured value (interpolated from the profiles at 430 and 1400 MHz) of 17.9°. Similarly, the secondary-mode component pairs in Fig. 6 have the dimensions of an outer cone—twice $\rho_{\rm outer} = 5.75°/P^{\frac{1}{2}}$ or 24.1° which agrees very well with the observed value of $24.5° \pm 0.5°$.

We are then left with the well known conal component pair comprised by comps. 2 and 4 (I and III), which has a scaled 1-GHz width of only about 9.4° between the half power points. This pair is far too narrow to be an inner cone, so we are forced to consider the possibility that there exists a 'further-in' cone with a dimension of some $2.5°/P^{\frac{1}{2}}$. Some other examples of what may be pulsars with 'further-in' cones do exist; pulsar 1914+13 was encountered in Paper VI and several pulsars falling along such a track can be identified in the work of Gil *et al.* (1993) and Kramer *et al.* (1994). We hardly need to point out that the small dimensions of such conal pairs and their proximity both to core components and to inner conal component pairs, make their identification difficult, and we would expect to encounter them only in some few exceptional circumstances.

These identifications seem to completely resolve the basic question of pulsar 1929+10's emission geometry—but at the cost of abandoning the implications of the single-vector model for this pulsar. We cannot therefore use the SVM to determine its magnetic latitude α and sight-line impact angle β, but the pulsar exhibits core widths and conal emission radii which are completely compatible with those which would be expected for a two-pole interpulsar—that is, α near 90° and β near 0°. A number of circumstances are discussed above which might compromise the PA traverse in pulsars **a**) with small impact angles and **b**) with equatorial emission geometries. It appears that in 1929+10 we encounter both circumstances.

This said, we are left with two fascinating and potentially important questions: how is it that some pulsars emit a core beam and a *triple* set of concentric conal beams? Further, how is it that two of the conal beams—those characterized by the primary polarisation-mode emission—are concentric and symmetrical about the core component, whereas the other one—which is characterized by the secondary-mode emission—is assymetric and greatly displaced to earlier longitudes? It would seem that we have stumbled on some very interesting evidence for a propagation phenomenon in the pulsar magnetosphere.

12. Summary and conclusions: Polarisation structure

Pulsar 1929+10 exhibits nearly completely linearly polarised emission over most of its rotation cycle. At no longitude are we able to say that it is precisely complete, but at some points, where the polarisation is high and the statistics are favorable, the observed fractional linear exceeds 97%. Whether this is a significant statement about depolarisation, given the 'pedestal' polarisation issues discussed above, is difficult to say. Certainly there are few other pulsars with such high and consistent linear polarisation as 1929+10. The Vela pulsar is a possible competitor, but no thorough

study based on sufficiently well calibrated polarimetry has yet been carried out, so that one can only venture a guess. As a polarisation calibrator, 1929+10 is in a class by itself.

It is paradoxical that a region near the boundary of MP comps. 3 and 4 exhibits rather less linear, and it is here that one can ask interesting questions about the processes which lead to its depolarisation. We have taken some care to study and model the emission in this region. Several different methods of polarisation-mode separation were used to delineate the properties of the two modes and to assess whether the process of depolarisation is compatible with the incoherent interference of two orthogonal, fully linearly polarised modes.

Study of the dynamical behaviour of the modal transition process shows that intervals of secondary-polarisation-mode dominance are infrequent and nearly randomly distributed. The transitions are rapid, and the emission usually switches back to the primary mode by the subsequent period. The transitions are also simultaneous over all the longitudes where significant orthogonal emission exists. Interestingly, there is a weak tendency for pulses with strong SPM emission to cluster or to follow each other two or three periods later.

We find that both the primary and secondary polarisation modes are rather steady in amplitude. The primary-mode amplitude distribution can be approximated by a χ^2 distribution of some 4 to 10 degrees of freedom. The secondary-mode distribution is also quite steady, but at a (1400-MHz) mean amplitude some twice as great as the primary-mode emission at the comp. 3/4 boundary. This latter distribution is not well modeled using a χ^2 PDF, but is more successfully modeled as being nearly constant in intensity, but sporadic. On the basis of these two distributions, it was possible to model the characteristics observed in this region; those pulses with a primary-mode PA are highly polarised and steady, whereas those pulses with a secondary-mode PA are depolarised, much stronger, and span a large range of intensity. We believe that our work provides reasonably strong evidence that the incoherent superposition of two fully polarised and orthogonal modes can account for the depolarisation observed in this pulsar.

Finally, we reiterate that this sporadic secondary-mode emission is identified with the more intense, trailing component of an outer conal component pair. The leading component of this cone is seen as the low level emission on the extreme leading edge of the MP. This trailing component occurs in longitude near the boundary of MP comps. 3 and 4—at the point of maximum depolarisation—but appears completely independent of these MP features. This remarkable overlapping of emission features may occur more generally, but most other cases are so complex that it is difficult to delineate what is happening. In 1929+10, the situation could not be clearer, because the secondary-mode emission is exclusively associated with the pulsar's outer conal emission. Theoretically, of course, we might expect different polarisation modes to have somewhat different propagation paths in the star's magnetosphere. Many people have looked for such effects but have found it difficult to identify them. In pulsar 1929+10 we seem to have encountered what may be a *bona fide* example of a propagation effect in the pulsar magnetosphere. It remains to be seen whether the ·isting plasma theory (i.e., Barnard & Arons 1986 or Asseo 1995) is compatible h what we have observed.

ıs a two-pole interpulsar 1929+10 exhibits more emission regions than just those ɔciated with its MP and IP. In particular, its PC component has long been known

and now apparently assumes a larger significance. We noted in our previous paper on pulsar 0823+26 (Rankin & Rathnasree 1995) that all known PCs seem to follow the MP core component (apparently, there are no 'precursors' in this sense, only 'postcursors'—and this includes the misnamed component in the Crab pulsar's profile). Further, though the statistics are yet small, it seems that all PC components occur in pulsars with a nearly orthogonal magnetic geometry—that is, $\alpha \sim 90°$. Pulsar 0823+26 provided one such example, 1929+10 is a second, and 2217+47 (Suleymanova & Shitov 1994) may well provide a third. We noted that it is only for such pulsars that there is a bundle of trailing equatorial field lines which have a tangent in the direction of the observer's sight line for a significant portion of the star's rotation cycle.

The remarkable 'notches' seen in the 430-MHz PC component are seemingly a new phenomenon not seen in the profiles of other pulsars. However, we have learned that a pair of very similar features is also seen in the profile of millisecond pulsar J0437–4715 (Navarro 1996). Here they follow the MP peak by about 70° (as opposed to some 100° in 1929+10) and their position is independent of frequency over more than an octave. Clearly, there are rather few pulsars with emission of any kind so far from the MP and IP, so the phenomenon might turn out to be a quite usual feature of those few stars with emission at such unusual longitudes. We have no idea whatsoever about what might be the cause of these distinct 'notches'.

We have not begun to exhaust the rich and abundant phenomena in the emission of our local 'neighbor' pulsar 1929+10, but we hope that this study will prove interesting and useful to those engaged in trying to understand the physical basis of pulsar radiation.

Acknowledgements

We thank Amy Carlow, Vera Izvekova, Svetlana Suleymanova, and Kyriaki Xilouris for help with the 1992 observing, Phil Perillat for his remarkable software for the Arecibo 40-MHz Correlator, and Avinash Deshpande for his fluctuation-spectrum analysis. The paper has greatly benefitted from the comments and critiques of our colleagues; we therefore want to thank Don Backer, Dipankar Bhattacharya, Jim Cordes, Avinash Deshpande, Tim Hankins, Mark McKinnon, V. Radhakrishnan, and Joel Weisberg for helpful discussions and/or probing questions about our various analyses and interpretations. One of us (JMR) also wishes to acknowledge the support of the U. S. Educational Foundation in India and the hospitality of the Raman Research Institute, where much of this work was carried out both while she was in residence on a Fulbright Fellowship and during several subsequent visits. This work was supported in part by grants from the U. S. National Science Foundation (AST 89–17722 and INT 93–21974). Arecibo Observatory is operated by Cornell University under contract to the U. S. National Science Foundation.

References

Abramowitz, M., Stegun, I. A. 1965, Handbook of Mathematical Functions (Dover: New York).
Asseo, E. 1995, *Mon. Not. R. Astr. Soc.*, **276**, 74.
Backer, D. C. 1970, *Nature* (*London*), **228**, 42.

Backer, D. C. 1971, Ph. D. thesis, Cornell University.
Backer, D. C. 1973, *Astrophys. J.*, **182**, 245.
Backer, D. C. 1976, *Astrophys. J.*, **209**, 895.
Backer, D. C., Rankin, J. M. 1980, *Astrophys. J. Suppl.*, **42**, 143.
Barnard, J. J., Arons, J. 1986, *Astrophys. J.*, **302**, 138.
Bartel, N., Sieber, W., Wielebinski, R. 1978, *Astr. Astrophys.*, **68**, 361.
Blaskiewicz, M., Cordes, J. M., Wasserman, I. 1991, *Astrophys. J.*, **370**, 643.
Cordes, J. M. 1997, private communication.
Cordes, J. M., Rankin, J. M., Backer, D. C. 1978, *Astrophys. J.*, **223**, 961.
Craft, H. D. E. 1969, *CRSR Report No. 395* (Cornell University, Ithaca, New York).
Deshpande, A. A. 1997, private communication.
Gil, J. A. 1981, *Acta Physica Polonicae*, **B12**, 1081.
Gil, J. A., Kijak, J., Seiradakis, I. 1993, *Astr. Astrophys.*, **272**, 268.
Hagen, J. 1987, *NAIC Electronics Department Manual No. 8319.*
Hankins, T. H., Fowler, L. A. 1986, *Astrophys. J.*, **304**, 256.
Hankins, T. H., Rankin, J. M. 1994, private communication.
Hankins, T. H., Rickett, B. J. 1986, *Astrophys. J.*, **311**, 684.
Hewish, A., Bell, S. J., Pilkington, J. D. H., Scott, P. F., Collins, R. A. *Nature* (*London*), **217**, 709.
Izvekova, V. A., Malofeev, V. M., Shitov, Yu. P. 1989, *Sov. Astron.*, **33**, 175.
Jones, P. B. 1980, *Astrophys. J.*, **236**, 661.
Kramer, M. 1994, *Astr. Astrophys.*, **107**, 527.
Kramer, M., Wielebinski, R., Jessner, A., Gil, J. A., Seiradakis, J. A. 1994, *Astr. Astrophys. Suppl. Ser.*, **107**, 515.
Komesaroff, M. M. 1970, *Nature* (*London*), **225**, 612.
Large, M. I., Vaughan, A. E., Wielebinski 1968, *Nature* (*London*), **220**, 753.
Lyne, A. G., Manchester, R. N. 1988, *Mon. Not. R. Astr. Soc.*, **234**, 477.
Manchester, R. N., Taylor, J. H. 1977, *Pulsars* (Freeman: San Francisco).
Manchester, R. N., Taylor, J. H., Huguenin, G. R. 1973, *Astrophys. J. Lett.*, **179**, L7.
Manchester, R. N., Taylor, J. H., Huguenin, G. R. 1975, *Astrophys. J.*, **196**, 83.
Mitra, D., Deshpande, A. A. 1997, private communication.
Moran, J. M. 1976, *Methods of Experimental Physics*, **12C**, 228.
Morris, D., Graham, D. A., Sieber, W., Bartel, N., Thomasson, P. 1981, *Astr. Astrophys. Suppl. Ser.*, **46**, 421.
Narayan, R., Vivekanand, M. 1982, *Astr. Astrophys.*, **113**, L3.
Navarro, J. 1996, in *Proceedings of the IAU Colloquium #160*, Sydney, Australia, January 1996, Astronomical Society of the Pacific.
Nowakowski, L., Usowicz, J., Kepa, A., Wolszczan, A. 1982, *Astr. Astrophys.*, **116**, 158.
Perillat, P. 1988, *NAIC Computer Department Report #23.*
Perillat, P. 1992, private communication.
Perry, T. E., Lyne, A. G. 1985, *Mon. Not. R. Astr. Soc.*, **212**, 489.
Phillips, J. A. 1990, *Astrophys. J. Lett.*, **361**, L57.
Pilkington, J. D. H., Hewish, A., Bell, S. J., Cole, T. W. 1968, *Nature* (*London*), **218**, 126.
Press, W. H., Flannery, B. P., Teukolsky, S. A., Vetterling, W. T. 1986, *Numerical Recipes* (Cambridge Univ. Press; Cambridge).
Radhakrishnan, V., Cooke, D. J. 1969, Ap. Lett., **3**, 225.
Ramachandran, R., Deshpande, A. A. 1997, private communication
Rankin, J. M. 1983a, *Astrophys. J.*, **274**, 333. (Paper I)
Rankin, J. M. 1983b, *Astrophys. J.*, **274**, 359. (Paper II)
Rankin, J. M. 1986, *Astrophys. J.*, **301**, 901. (Paper III)
Rankin, J. M. 1990, *Astrophys. J.*, **352**, 247. (Paper IV)
Rankin, J. M. 1993a, *Astrophys. J.*, **405**, 285. (Paper VIa)
Rankin, J. M. 1993b, *Astrophys. J. Suppl*, **85**, 145. (Paper VIb)
Rankin, J. M., Benson, J. M. 1981, *Astr. J.*, **86**, 418.
Rankin, J. M., Campbell, D. B., Spangler, S. 1975, *NAIC Report #46.*
Rankin, J. M. Rathnasree, N. 1995, *J. Astrophys. Astr.*, 16, 327.
Rankin, J. M., Rathnasree, N., Xilouris, K. 1998, in preparation.

Rankin, J. M., Stinebring, D. R., Weisberg, J. M. 1989, *Astrophys. J.*, **346**, 869.
Rankin, J. M., Wolszczan, A., Stinebring, D. R. 1988, *Astrophys. J.*, **324**, 1048.
Ritchings, R. T. 1976, *Mon. Not. R. Astr. Soc.*, **176**, 249.
Sieber, W., Reinecke, R., Wielebinski, R. 1975, *Astr. Astrophys.*, **38**, 169.
Stinebring, D. R., Cordes, J. M., Rankin, J. M., Weisberg, J. M., Boriakoff, V. 1984a, *Astrophys. J. Suppl.*, **55**, 247.
Stinebring, D. R., Cordes, J. M., Weisberg, J. M., Rankin, J. M., Boriakoff, V. 1984b, *Astrophys. J. Suppl.*, **55**, 279.
Suleymanova, S. A., Shitov, Yu. P. 1994, *Astrophys. J. Lett.*, **422**, L17.
Tauris, T. M., Nicastro, L., Johnston, S., Manchester, R. N., Bailes, M., Lyne, L. G., Glowacki, J., Lorimer, D. R., D'Amico N. 1994, *Astrophys. J. Lett.*, **428**, L53.
Taylor, J. H., Huguenin, G. R. 1971, *Astrophys. J.*, **167**, 273.
Taylor, J. H., Manchester, R. N., Huguenin, G. R. 1975, *Astrophys. J.*, **195**, 513.
Wielebinski, R., Jessner, A., Kramer, M., Gil, J. A. 1993, *Astr. Astrophys.*, **272**, L13.
Xilouris, K. M., Seiradakis, J. M., Gil, J., Sieber, W., Wielebinski, R. 1995, *Astr. Astrophys.*, **293**, 153.